

Fluctuations in solidification

Alain Karma

Physics Department, Northeastern University, Boston, Massachusetts 02115

(Received 15 January 1993)

We present an analytical treatment of (i) the incorporation of thermal noise in the basic continuum models of solidification, (ii) fluctuations about nonequilibrium steady states, and (iii) the amplification of noise near the onset of morphological instability. In (i), we find that the proper Langevin formalism, consistent with both bulk and interfacial equilibrium fluctuations, consists of the usual bulk forces and an extra stochastic force on the interface associated with its local kinetics. At sufficiently large solidification rate, this force affects interfacial fluctuations on scales where they are macroscopically amplified and, thus, becomes relevant. An estimate of this rate is given. In (ii), we extend the Langevin formalism outside of equilibrium to characterize the fluctuations of a stationary and a directionally solidified planar interface in a temperature gradient. Finally, in (iii), we derive an analytic expression for the linear growth of the mean-square amplitude of fluctuations slightly above the onset of morphological instability. The amplitude of the noise is found to be determined by the small parameter $k_B T_E d_0^c l_T / \gamma \lambda_c^4$ where γ is the surface energy, d_0^c is the chemical capillary length, l_T is the thermal length, and λ_c is the critical wavelength. Possible applications to experiment are discussed.

PACS number(s): 61.50.Cj, 05.70.Ln, 64.70.Dv, 81.30.Fb

I. INTRODUCTION AND SUMMARY

A. Background

Thermodynamic fluctuations (thermal noise) inherent in bulk matter are, in most situations, much too weak to affect the dynamics of patterns which arise spontaneously in nonequilibrium systems. However, they can have an important effect in situations where they become amplified to a macroscopic scale by intrinsic linear instabilities [1].

In solidification, the pronounced sidebranching activity observed during dendritic solidification of alloys is of considerable metallurgical relevance. The intricate tree-like structure which results from this activity determines the solute microsegregation pattern of the solidified material which in turn largely controls its mechanical properties. This activity, according to our present theoretical understanding [2–7], seems remarkably to result in the vast majority of experiments in both pure materials [8] and alloys [9] (but not all [10]) from the amplification of tiny perturbations of the interface triggered by some form of noise. Another important place, pointed out recently by Warren and Langer (WL) [11], where noise seems to play an important role is in the selection of the primary spacing of dendritic arrays in directional solidification [12–14]. There, the noise determines indirectly the initial wavelength of a transient cellular array structure which evolves via a complicated cell elimination (coarsening) process towards a stable dendritic array structure [11].

The precise physical origin of noise in these examples, or even its relevance, remains uncertain. In the case of dendritic sidebranching, the present uncertainty in its origin is due to a quantitative calculation by Langer [5] which has indicated that purely thermal noise is probably not strong enough to account for the observed sidebranch

amplitude in the experiment of Huang and Glicksman [8]. In the case of directional solidification, the present situation seems somewhat less conflictual and the theory is more tractable. This is due to the fact that calculations of noise amplification involve fluctuations about a planar interface and do not suffer the complications associated with three-dimensional anisotropic needle crystals. In a quantitative calculation using thermal noise WL have found a relatively good agreement with experiment [12, 13] for the initial wavelength of the transient cellular array structure. It should be mentioned, however, that in the related problem of the onset of the dendritic instability the role of thermal noise remains less clear [15, 16]. In one experiment [15], an initially stationary planar interface between a cold and a hot contact (i.e., effectively in a temperature gradient) was progressively undercooled by lowering the temperature of the hot contact, thereby allowing a morphological instability to develop. On the basis of a rough theoretical estimate, Qian *et al.* [16] first concluded that thermal noise was of about the right magnitude to account for the rise of the instability in this experiment. However, a more rigorous calculation mentioned in a note added in proof by the same authors [16] led to the opposite conclusion, namely, that thermal noise was several orders of magnitude too small to account for this rise.

Eventually, it will probably become necessary to consider other sources of noise which could be related, for example, to the presence of grain boundaries, to the presence of small foreign particles including microbubbles [17, 18], or to other extrinsic effects inherent in the experimental setup. It remains that thermal fluctuations, in contrast to the above sources, represent the most natural and “unavoidable” source of noise. For both fundamental and practical reasons, it therefore seems essential at present to invest some effort in developing a better

theoretical understanding of these fluctuations. In this paper, I shall present the results of analytical studies in this direction which have three main goals.

(1) The first is to develop a self-consistent Langevin formalism for incorporating thermal noise in the usual continuum models of solidification [19] defined on a hydrodynamic scale with a sharp two-phase boundary (a summary of this formalism was reported in Ref. [20]).

(2) The second is to provide a detailed characterization of the nonequilibrium fluctuations (in particular the fluctuation spectrum $\langle \xi_{\mathbf{k}} \xi_{-\mathbf{k}} \rangle$) of a stationary and a steady-state moving planar interface in a temperature gradient. At a practical level, this characterization is an essential prerequisite to study the amplification of fluctuations by morphological instability [21] in directional solidification, both in the example considered by WL and other experimental situations. At a more fundamental level, it also provides a basis of comparison with (i) a potential calculation of nonequilibrium (long-wavelength) interfacial fluctuations starting from a fully microscopic model which could serve as a check of the validity of the Langevin formalism outside of equilibrium, and (ii) experimental measurements of this spectrum.

(3) The third is to provide an analysis of the amplification of thermal noise *near* the onset of morphological instability in directional solidification. This analysis yields an analytical prediction of the linear growth (in time) of the mean-square amplitude of interfacial fluctuations. In an experimental setting, this prediction could be used to determine the amplitude of the noise by measuring the time necessary for fluctuations to become macroscopically amplified and, hence, infer its origin.

The present procedure [5, 11] used to incorporate thermal fluctuations was first introduced by Cherepanova [22] and consists of adding to the diffusion equations stochastic Langevin forces, uncorrelated in space and time, chosen to reproduce the known *bulk* equilibrium fluctuations of temperature and concentration in each phase separately. For this procedure to be correct, it must also reproduce the known equilibrium interfacial fluctuations that is, the fluctuations of the boundary separating the two phases on scales much larger than the microscopic interface width. Two somewhat separate issues arise in relation to the first goal outlined above.

(i) The first, raised recently by WL, pertains to the fact that the procedure of Cherepanova assumes that the boundary has no net effect on bulk forces. While this seems at least intuitively correct for the symmetric model where both phases have the same bulk thermodynamic properties it is not *a priori* obvious why the same should be true of the more general case where the two phases have distinct thermodynamic properties.

(ii) The second pertains to the fact that the usual Gibbs-Thomson condition implicitly assumes that the interface adjusts its position *instantaneously* in response to a given temperature or concentration fluctuation. Atomically rough interfaces (to which we restrict our attention) relax exponentially in time via a first order kinetics usually incorporated by adding a term linear in velocity to the Gibbs-Thomson condition. Such a term was actually included in the basic equations considered by

Cherepanova. However, what was not included is an extra stochastic force, separate from bulk forces, which seems necessary to compensate for the extra source of dissipation associated with the relaxational kinetics of the interface. Since the effect of the latter becomes progressively more important with increasing velocity one would also expect the effect of this extra force to increase with velocity. However, when precisely does it become relevant? This question is particularly relevant in view of the fact that dendritic sidebranching, for example, is observed to persist over velocities ranging from a few micrometers per second to several meters per second [23].

B. Results

In Sec. II of this paper, we develop a Langevin formalism, consistent with both bulk and interfacial fluctuations, which resolves these two issues. We find that bulk forces, alone, suffice to reproduce the correct equilibrium interfacial fluctuations in the absence of interface kinetics; and, hence, that the interface has effectively no net effect on these forces. An expression for the nonconserved “interface force” necessary to generate the correct fluctuations in the presence of interface kinetics is derived.

In Sec. III, we investigate the relevance of the interface force to the formation of solidification patterns. This analysis is not specific to any particular experiment but is aimed at estimating, quite generally, at what velocity v^* this force starts to affect interfacial fluctuations on scales where they are selectively amplified by linear instabilities. This velocity can be interpreted as the velocity of a dendrite tip in the context of sidebranching. To do so we first calculate the crossover scale λ^* below which the interface force affects the equilibrium fluctuation spectrum (see Fig. 1). We then determine v^* by comparing this scale to the usual stability length λ_S which sets the scale of the short-wavelength cutoff below which fluctuations are not amplified.

For the case of a pure substance, this procedure yields the value $\lambda^* \sim cD_T/\mu L$ and the estimate, $v^* \sim \mu^2 \gamma T_M / cD_T$, where μ (m/sec K) is the kinetic coefficient, γ (J/m²) is the surface energy, c (J/K m³) is the specific heat per unit volume, L (J/m³) is the latent heat per unit volume, T_M (K) is the melting temperature, and D_T (m²/sec) is the thermal diffusivity (an analogous expression for the case of alloys is also derived). For materials with fast kinetics, such as monatomic metals, the value of v^* obtained using current theoretical estimates of μ [24] is on the order of m/sec. While, for materials with large molecules and slower kinetics, v^* could be considerably smaller (perhaps as small as in the 1–100- μ m/sec range). However, it is presently difficult to give a reliable estimate for these materials given the lack of precise knowledge of the kinetic coefficient. The main conclusion is that the interface force should be relevant in rapid solidification of metallic alloys, potentially being responsible for sidebranching, and perhaps even at slower growth rate for materials with slow kinetics.

In Sec. IV, we study the fluctuations of a stationary and a moving planar interface in a temperature gradi-

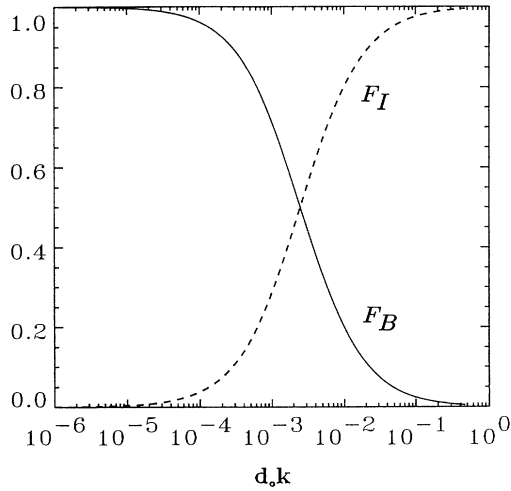


FIG. 1. Plot of $F_B(d_0 k; \bar{\mu})$ (solid line) and $F_I(d_0 k; \bar{\mu})$ (dashed line) for the symmetric model of the solidification of a pure substance with $\bar{\mu} = \mu\Gamma/D_T = 5 \times 10^{-3}$. The equilibrium interfacial fluctuation spectrum $\langle \xi_{\mathbf{k}} \xi_{-\mathbf{k}} \rangle = k_B T_M / \gamma k^2$ with both bulk and interface forces. With only the former $\langle \xi_{\mathbf{k}} \xi_{-\mathbf{k}} \rangle = (k_B T_M / \gamma k^2) F_B(d_0 k; \bar{\mu})$ and with only the latter $\langle \xi_{\mathbf{k}} \xi_{-\mathbf{k}} \rangle = (k_B T_M / \gamma k^2) F_I(d_0 k; \bar{\mu})$. The consistency of the Langevin formalism requires $F_B(d_0 k; \bar{\mu}) + F_I(d_0 k; \bar{\mu}) = 1$. The crossover wavevector k^* is determined by the intersection of the two curves.

ent. To do so we extend the Langevin formalism outside of equilibrium by making the usual assumption that the magnitude of the local forces is determined by the local values of the corresponding thermodynamic variables (temperature and concentration). Outside of solidification, Tremblay, Siggia, and Arai [25] have actually tested the validity of this assumption for a single bulk phase in a temperature gradient and a particular choice of microscopic model. In the case of solidification, performing a fully microscopic calculation would represent a formidable task which we do not undertake here. We expect that the extension of the Langevin formalism should be quite accurate to characterize interfacial fluctuations at relatively small growth rate (in the 1–100- $\mu\text{m}/\text{sec}$ range). At large solidification rate, this extension is likely to break down. However, at present, we cannot tell at what growth rate this breakdown may occur and how nonequilibrium fluctuations will become modified. Answering this question, which is crucial for a fundamental understanding of rapid solidification, remains a difficult challenge for future investigations.

The fluctuation spectrum, $\langle \xi_{\mathbf{k}} \xi_{-\mathbf{k}} \rangle_G$, of a stationary planar interface in a temperature gradient is shown in Fig. 2. This plot is for the symmetric model [19] of a pure substance; the analogous spectrum for a model of alloy solidification that includes both temperature and concentration fields is essentially identical. This spectrum can be shown analytically to have the asymptotic forms $\langle \xi_{\mathbf{k}} \xi_{-\mathbf{k}} \rangle_G \cong k_B T_E / \gamma (k^2 + a^{-2})$ for $k \gg b^{-1}$, and $\langle \xi_{\mathbf{k}} \xi_{-\mathbf{k}} \rangle_G \cong k_B / 2 c k$ for $k \ll b^{-1}$, where $b = T_E / G$ and $a = (\gamma T_E / LG)^{1/2}$. The first form reflects the pinning effect of the temperature gradient on scales larger than a . It is directly analogous to the effect of gravity on a

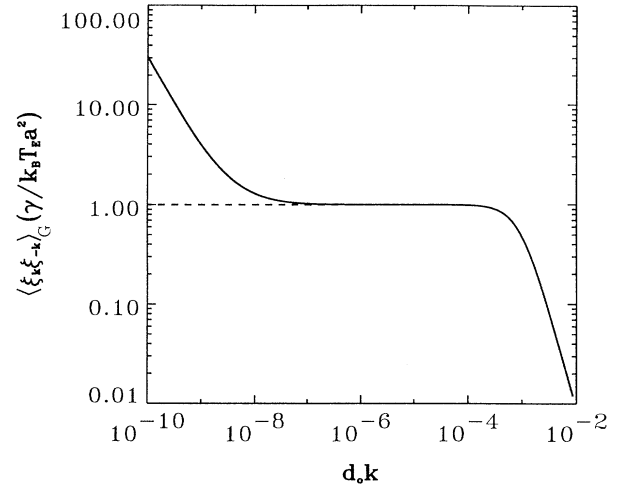


FIG. 2. Interfacial fluctuation spectrum of a stationary planar interface in a temperature gradient (SCN with $G = 100$ K/cm).

liquid-gas system and can be alternatively derived using fluctuation theory. The second form reflects a fluctuation enhancement on scale larger than b which originates from the temperature dependence of the bulk Langevin force associated with the temperature field.

For typical experimental values of G in the 10–100-K/cm range, b is in the mm to cm range, $a = (\gamma T_E / LG)^{1/2}$ is in the micrometer range, and the range of wavevector which becomes amplified by morphological instabilities falls inside the plateau of the fluctuation spectrum in Fig. 2. This is clearly seen in Fig. 3, which shows a typical plot of the fluctuation spectrum $\langle \xi_{\mathbf{k}} \xi_{-\mathbf{k}} \rangle_v$ of a steady-state moving planar interface. In the small velocity limit, this spectrum reduces to that

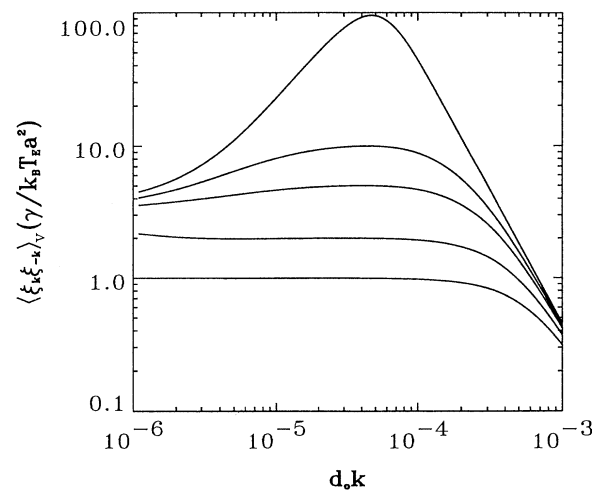


FIG. 3. Interfacial fluctuation spectrum of a directionally solidified planar interface below the onset of morphological instability for $v/v_c = 0.0, 0.5, 0.8, 0.9,$ and 0.99 . (SCN-0.10 wt % acetone alloy with $G=38.2$ K/cm).

of the stationary case of Fig. 2 and, slightly below onset, it exhibits the usual enhancement of fluctuation ($\langle \xi_{\mathbf{k}_c} \xi_{-\mathbf{k}_c} \rangle_v \sim 1/[v_c - v]$). Trivedi and Somboonsuk, in a directional solidification experiment [12], have observed a second spatial periodicity in the transient cellular array structure with a wavelength λ'_0 (in the 0.2–0.5-mm range) which is about an order of magnitude larger than the wavelength λ_0 usually associated with the Mullins-Sekerka instability. This observation, however, cannot be explained in terms of the present small k enhancement of the fluctuation spectrum shown in Fig. 2. This is because, in their experiment, the corresponding value of b ($\simeq 5$ cm) is about an order of magnitude larger than λ'_0 . Generally, b is always much larger than the scale over which cellular structures are formed. Thus, the small k enhancement, although interesting in itself, should not play a significant role in directional solidification.

Finally, in Sec. V, we investigate the effect of thermal noise close to the onset of morphological instability. The main result is an analytical expression for the “amplification time” t_A necessary for thermal fluctuations to become macroscopically amplified (i.e., for the amplitude of the cellular structure to become comparable to its wavelength) after the pulling speed of the sample is suddenly changed from a value v_0 , slightly less than the onset velocity v_c , to a value v_1 slightly larger than v_c . This time is defined implicitly by the relation

$$t_A \cong \frac{\tau_D}{2 c_2 [v_c/v_1 - 1]} \ln \left[\frac{F}{\sqrt{t_A/\tau_D}} \left(\frac{1}{1 - v_0/v_c} + \frac{1}{1 - v_c/v_1} \right) \right], \quad (1)$$

which is valid for $t_A/\tau_D \gg 1/c_2[1 - v_c/v_1]$ and $c_2[1 - v_c/v_1] \ll 1$. $F = k_B T_E d_0^c l_T / \gamma \lambda_c^4$ is a small parameter typically in the range 10^{-12} – 10^{-16} which is a dimensionless measure of the amplitude of the noise, d_0^c and l_T are the chemical capillary length and thermal length (Sec. IV B), and c_2 is a constant which is determined by the form of the linear growth rate of instability near onset [i.e., $\omega(k_c; v) \tau_D \cong c_2(1 - v_c/v)$].

In the Bénard convection analog [27, 28], the small parameter $F = k_B T / \rho d \nu^2$ is the ratio of a microscopic thermal fluctuation energy $k_B T$ and a macroscopic dissipative energy $(\rho d^3)(\nu/d)^2$, where ρ is the mass density, ν the kinematic viscosity, and d the plate separation. Here, the physically meaningful quantity is actually the square root of F which can be written as the product of two ratios of length scales

$$F^{1/2} = \frac{(k_B T_E / \gamma)^{1/2}}{\lambda_c} \frac{(d_0^c l_T)^{1/2}}{\lambda_c}. \quad (2)$$

The first is directly analogous to the convection ratio with length instead of energy and accounts for most of the smallness of the parameter F . In particular, it involves the ratio of a microscopic length $(k_B T_E / \gamma)^{1/2}$ of the order of angstroms, which sets the scale of equilibrium interfacial fluctuations and λ_c . The second factor is the ratio of two mesoscopic lengths $a = (d_0^c l_T)^{1/2}$, which is the same scale a which enters in the fluctuation

spectra $\langle \xi_{\mathbf{k}} \xi_{-\mathbf{k}} \rangle_G$ and $\langle \xi_{\mathbf{k}} \xi_{-\mathbf{k}} \rangle_v$, and λ_c . Physically, it accounts for the fact that the temperature gradient reduces dramatically the amplitude of interfacial fluctuations on scales larger than a (Figs. 2 and 3). This ratio is typically in the range 10^{-3} – 10^{-2} in directional solidification experiments.

Equation (1) is the main result of this paper with regard to experiment. It provides a rigorous basis to test if thermal noise is the dominant noise source in a precise directional solidification experiment near onset by measuring the time necessary for fluctuations to become macroscopically amplified. This result is not easily applicable to standard experiments on binary alloys because the velocity window close to v_c where it is strictly valid is in general too narrow to be studied reliably. Nonetheless, a theoretical estimation given at the end of Sec. V indicates that this window ought to be experimentally accessible with extremely dilute solutions or liquid-crystal systems.

II. LANGEVIN FORMALISM

A. Equilibrium fluctuations

The static thermodynamic properties are described by the grand potential

$$\Omega = -P_L(T, \mu_L) V_L - P_S(T, \mu_S) V_S + \gamma A, \quad (3)$$

where the subscripts S and L refer respectively to the solid and liquid phases, μ_ν ($\nu = L, S$) denotes the chemical potential of the solute in each phase, γ denotes the surface energy, V_ν ($\nu = L, S$) denotes the volume of each phase, and A denotes the interfacial area. There are two important relations, directly derivable from Eq. (3), which we shall use here. The first is the usual Gibbs-Thomson interfacial equilibrium condition

$$T_I = T_E - \Gamma \kappa \quad (4)$$

obtained by requiring that $\delta\Omega = 0$ at fixed total volume $V_S + V_L = V$. Here, T_I denotes the interface temperature, $T_E = T_M - m_E C_L$ the equilibrium melting temperature of the alloy, T_M the equilibrium melting temperature of the pure substance, C_L the equilibrium composition on the liquid side defined as the number of molecules per unit volume, m_E the absolute value of the slope of the liquidus, K_E the partition coefficient, $\Gamma = \gamma T_E / L$ the Gibbs-Thomson coefficient, and L the latent heat of melting per unit volume. The second is the Clausius-Clapeyron relation for dilute alloys

$$\frac{k_B T_E^2}{L} = \frac{m_E}{1 - K_E} \quad (5)$$

derived by differentiating Eq. (3) along the solid-liquid coexistence line [19].

According to the basic principles of statistical physics, the probability of a given fluctuation is given by

$$p(\alpha) = \frac{1}{Z} \exp \left(-\frac{W[\alpha]}{k_B T_E} \right), \quad (6)$$

where $Z \equiv \int \mathcal{D}\alpha \exp(-W[\alpha]/k_B T_E)$, and $W[\alpha]$ repre-

sents the minimum work required to carry out reversibly changes in thermodynamic quantities (α) from their average equilibrium values (α^*). The fluctuations of temperature and concentration in a small volume ΔV are then obtained by expressing W in terms of these variables [29]. The appropriate relations are

$$\langle \Delta T^2 \rangle = \frac{k_B T_E^2}{c_\nu}, \quad \nu = L, S \quad (7)$$

$$\langle (\Delta \bar{C}_\nu)^2 \rangle = \frac{k_B T_E}{N_\nu (\partial \mu_\nu / \partial \bar{C}_\nu)} = \frac{\bar{C}_\nu}{N_\nu}, \quad \nu = L, S, \bar{C}_\nu \ll 1 \quad (8)$$

where $\bar{C}_\nu = n_\nu / N_\nu$ denotes the solute concentration in each phase defined as the ratio of the number of solute and solvent molecules, and c_ν the specific heat per unit volume of each phase ($\nu = L, S$). Expressed in terms of the concentration per unit volume which we shall use in our calculations, Eq. (8) becomes

$$\langle (\Delta C_\nu)^2 \rangle = \frac{C_\nu}{\Delta V}, \quad \nu = L, S. \quad (9)$$

The minimum work required to deform the boundary between the two phases is given by

$$W = \gamma \delta A, \quad (10)$$

where δA is the total change in surface area of the boundary. This work can be written in the form

$$W[\xi] = \gamma \int d^2 r \left(\sqrt{1 + |\nabla_\perp \xi(\mathbf{r})|^2} - 1 \right), \quad (11)$$

where $\xi(\mathbf{r})$ denotes the vertical displacement of the interface from a reference (x, y) plane perpendicular to the z axis chosen such that $\langle \xi(\mathbf{r}) \rangle = 0$; \mathbf{r} and ∇_\perp denote respectively the two-dimensional position vector and gradient in this plane. We choose positive values of ξ to correspond to freezing (i.e., increasing V_S).

In general, interfacial fluctuations are sufficiently small such that only the first term in an expansion of the square root in Eq. (11) needs to be retained. The probability distribution of equilibrium interfacial fluctuations is then given by

$$p = \frac{1}{Z} \exp \left(-\frac{\gamma}{k_B T_E} \int d^2 r \frac{1}{2} |\nabla_\perp \xi(\mathbf{r})|^2 \right). \quad (12)$$

Next, using the definition

$$\xi(\mathbf{r}) = \int \frac{d^2 k}{(2\pi)^2} e^{i\mathbf{k}\cdot\mathbf{r}} \xi_{\mathbf{k}} \quad (13)$$

to Fourier transform the integral appearing in Eq. (12), we obtain after performing simple Gaussian integrations the mean-square interfacial fluctuation spectrum which takes the usual form

$$\langle \xi_{\mathbf{k}} \xi_{\mathbf{k}'} \rangle = (2\pi)^2 \delta(\mathbf{k} + \mathbf{k}') \frac{k_B T_E}{\gamma} \frac{1}{k^2} \quad (14)$$

or

$$\langle \xi_{\mathbf{k}} \xi_{-\mathbf{k}} \rangle = \int \frac{d^2 k'}{(2\pi)^2} \langle \xi_{\mathbf{k}} \xi_{\mathbf{k}'} \rangle = \frac{k_B T_E}{\gamma} \frac{1}{k^2}. \quad (15)$$

We conclude by recalling that the mean-square interfacial displacement diverges logarithmically with the size of the system

$$\langle \xi(\mathbf{r})^2 \rangle = \int \frac{d^2 k}{(2\pi)^2} \langle \xi_{\mathbf{k}} \xi_{-\mathbf{k}} \rangle = \frac{k_B T_E}{2\pi\gamma} \ln \frac{L_0}{\Lambda}, \quad (16)$$

where $L_x = L_y = L_0$ is the linear dimension of the surface, Λ is some short-wavelength cutoff scale comparable to a molecular diameter which fixes the maximum wavevector in the integral. As examples, for succinonitrile (SCN) and Al, the root-mean-square interfacial fluctuations of a 1-cm² crystal face are given by

$$\langle \xi^2 \rangle^{1/2} = \begin{cases} 12.2A & \text{for SCN} \\ 6.4 & \text{for Al} \end{cases}$$

where we have used $\Lambda = 1A$ and the materials parameter given in Ref. [30].

B. Langevin forces

We start by writing down the basic continuum equations describing the solidification of a dilute binary alloy, including all the necessary Langevin forces. We then investigate the consistency of this formalism with equilibrium fluctuations and discuss the physical relevance of its constitutive forces. These equations consist of the usual diffusion equations of heat and solute in each phase together with the respective conservation conditions and Gibbs-Thomson boundary condition at the interface:

$$\frac{\partial T_\nu}{\partial t} = D_\nu^T \Delta T_\nu - \nabla \cdot \mathbf{q}^{\nu,T}(\mathbf{R}, t), \quad \nu = L, S \quad (17)$$

$$L v_n = \hat{\mathbf{n}} \cdot [c_S D_S^T \nabla T_S - c_L D_L^T \nabla T_L] + \hat{\mathbf{n}} \cdot [c_L \mathbf{q}^{L,T}(\mathbf{p}) - c_S \mathbf{q}^{S,T}(\mathbf{p})], \quad (18)$$

$$\frac{\partial C_\nu}{\partial t} = D_\nu^C \Delta C_\nu - \nabla \cdot \mathbf{q}^{\nu,C}(\mathbf{R}, t), \quad \nu = L, S \quad (19)$$

$$C_L(1 - K_E)v_n = \hat{\mathbf{n}} \cdot [D_S^C \nabla C_S - D_L^C \nabla C_L] + \hat{\mathbf{n}} \cdot [\mathbf{q}^{L,C}(\mathbf{p}) - \mathbf{q}^{S,C}(\mathbf{p})], \quad (20)$$

$$T_I(\mathbf{p}) = T_M - m_E C_L - \Gamma \kappa - \frac{v_n}{\mu} + \eta(\mathbf{r}, t), \quad (21)$$

where T_I denotes the interfacial temperature, D_ν^T and c_ν denote the thermal diffusivity and specific heat of each phase, D_ν^C the solute diffusivity of each phase, and μ is the linear kinetic coefficient. Also, $\mathbf{R} \equiv x \hat{\mathbf{x}} + y \hat{\mathbf{y}} + z \hat{\mathbf{z}}$ is the three-dimensional position vector and $\mathbf{r} \equiv x \hat{\mathbf{x}} + y \hat{\mathbf{y}}$ is a two-dimensional vector in the (x, y) plane with the coordinate of the interface parametrized by $\mathbf{p} \equiv x \hat{\mathbf{x}} + y \hat{\mathbf{y}} + \xi(\mathbf{r}, t) \hat{\mathbf{z}}$. The three- and two-dimensional gradients are denoted, respectively, by $\nabla \equiv \partial_x \hat{\mathbf{x}} + \partial_y \hat{\mathbf{y}} + \partial_z \hat{\mathbf{z}}$ and $\nabla_\perp \equiv \partial_x \hat{\mathbf{x}} + \partial_y \hat{\mathbf{y}}$. Δ denotes the three-dimensional

Laplacian. The curvature κ and normal velocity v_n of the interface are defined by

$$\kappa = -\nabla_{\perp} \cdot \left(\frac{\nabla_{\perp} \xi(\mathbf{r}, t)}{[1 + |\nabla_{\perp} \xi(\mathbf{r}, t)|^2]^{1/2}} \right), \quad (22)$$

$$v_n = \frac{\partial \xi(\mathbf{r}, t)}{\partial t} \hat{\mathbf{n}} \cdot \hat{\mathbf{z}}. \quad (23)$$

Finally, the Gaussian random variables $\mathbf{q}(\mathbf{R}, t)$ and $\eta(\mathbf{r}, t)$, representing respectively the bulk forces and interface force, obey the correlations

$$\langle q_i^{\nu, T}(\mathbf{R}, t) q_j^{\nu, T}(\mathbf{R}', t') \rangle = 2 \frac{D_{\nu}^T k_B T_{\nu}(\mathbf{R}, t)^2}{c_{\nu}} \delta(\mathbf{R} - \mathbf{R}') \delta(t - t') \delta_{ij}, \quad \nu = L, S \quad (24)$$

$$\langle q_i^{\nu, C}(\mathbf{R}, t) q_j^{\nu, C}(\mathbf{R}', t') \rangle = 2 D_{\nu}^C C_{\nu}(\mathbf{R}, t)^2 \delta(\mathbf{R} - \mathbf{R}') \delta(t - t') \delta_{ij}, \quad \nu = L, S \quad (25)$$

$$\langle \eta(\mathbf{r}, t) \eta(\mathbf{r}', t') \rangle = 2 \frac{k_B T_I(\mathbf{p})^2}{\mu L} \frac{\delta(\mathbf{r} - \mathbf{r}') \delta(t - t')}{\sqrt{1 + |\nabla_{\perp} \xi(\mathbf{r}, t)|^2}}, \quad (26)$$

with $\delta(\mathbf{R} - \mathbf{R}') \equiv \delta(x - x')\delta(y - y')\delta(z - z')$, $\delta(\mathbf{r} - \mathbf{r}') \equiv \delta(x - x')\delta(y - y')$, and the factor of $[1 + |\nabla_{\perp} \xi(\mathbf{r}, t)|^2]^{1/2}$ in the denominator of Eq. (26) is necessary to ensure that the net force on a small area dS of the interface is independent of its orientation with respect to the (x, y) plane. Our present parametrization requires $\xi(\mathbf{r}, t)$ to be single-valued but the generalization to the more general case where $\xi(\mathbf{r}, t)$ is multivalued is straightforward. In equilibrium, the variances of the forces are constant with, respectively, $T_I(\mathbf{p}) = T(\mathbf{R}, t) = T_E$, $C_L(\mathbf{R}, t) = C_{\infty}$, and $C_S(\mathbf{R}, t) = K_E C_{\infty}$, where C_{∞} denotes here the alloy composition in the bulk liquid. Outside of equilibrium, they are determined by the local values of temperature and concentration, as denoted in Eqs. (24)–(26), following the usual assumption of local thermodynamic equilibrium.

There are two differences between the above equations and those originally written down by Cherepanova [22] which are worth pointing out. Firstly, in Cherepanova's formulation, bulk forces were omitted from the heat and solute conservation conditions. However, there is no *a priori* reason for their omission and, as we shall see below, their inclusion is needed for the formalism to be consistent with equilibrium fluctuations. Secondly, an extra stochastic interface force, absent in Cherepanova's formulation, has been added to the right-hand side of Eq. (21). This force is essential to compensate for the extra source of dissipation associated with the relaxational kinetics of the interface. A simple, albeit nonrigorous, way to see this is to consider the interfacial fluctuations generated by Eq. (21), alone, with the temperature and concentration frozen to their bulk equilibrium values. In this case, Eq. (21) once linearized about a flat interface simply becomes

$$\frac{1}{\mu} \frac{\partial \xi}{\partial t} = \Gamma \nabla_{\perp}^2 \xi + \eta(\mathbf{r}, t), \quad (27)$$

which, using Eq. (26), is trivially shown to generate the correct interfacial fluctuation spectrum given by Eq. (15). A more rigorous analysis presented in Sec. III, which takes into account simultaneously bulk and interfacial fluctuations, yields the same result.

C. Connection with equilibrium fluctuations by direct calculation

We now explore the first issue of whether the boundary has an effect on bulk forces. One of the most direct ways to resolve this issue is to calculate the interfacial fluctuation spectrum using the equations written above and check if it agrees with the equilibrium spectrum. For simplicity, we perform this calculation for the isothermal case without temperature fluctuations and without interface kinetics. The separate issues associated with the interface force are addressed in Sec. III. The corresponding equations are then given by Eqs. (19) and (20) together with the Gibbs-Thomson condition

$$C_L = C_{\infty} - \frac{\Gamma}{m_E} \kappa \quad (28)$$

and the noise correlation defined by Eq. (25) with $C_L(\mathbf{R}, t) = C_{\infty}$ and $C_S(\mathbf{R}, t) = K_E C_{\infty}$. The analogous calculation for a pure substance is essentially identical and the one for the coupled thermal-solutal problem is unnecessarily complicated for the present purposes. Also for shortness of notation, the superscript referring to the concentration field is dropped on the definition of the diffusivities and bulk forces.

To calculate the fluctuation spectrum we proceed as follows. We rewrite the basic equations of the model in terms of two coupled integral equations (one for each phase) using the standard Green's function boundary integral method. We then linearize these equations about a stationary planar interface and calculate $\langle \xi_{\mathbf{k}\omega} \xi_{\mathbf{k}'\omega'} \rangle$ by Fourier transform using the definition

$$\xi(\mathbf{r}, t) = \frac{1}{(2\pi)^3} \int d\omega d^2k e^{i(\mathbf{k}\cdot\mathbf{r} + \omega t)} \xi_{\mathbf{k}\omega}. \quad (29)$$

The static spectrum is then obtained via the identity

$$\langle \xi_{\mathbf{k}} \xi_{-\mathbf{k}} \rangle = \frac{1}{(2\pi)^4} \int d\omega d\omega' d^2k' \langle \xi_{\mathbf{k}\omega} \xi_{\mathbf{k}'\omega'} \rangle. \quad (30)$$

The calculations are lengthy but straightforward and their details are reported in Appendix A. The final result can be expressed in terms of an integral over the dimensionless frequency $\Omega = \omega/(D_L k^2)$:

$$g(\Omega) = \frac{\Gamma k}{m_E C_\infty (1 - K_E)} \left[\left(1 + i\Omega \right)^{1/2} + K_E \frac{D_S}{D_L} \left(1 + i\Omega \frac{D_L}{D_S} \right)^{1/2} \right] + i\Omega. \quad (32)$$

The integral over Ω on the right-hand side of Eq. (31) can then be shown to always equal unity [31], independently of the value k and all other constants appearing in $g(\Omega)$. Finally, combining this result with the Clausius-Clapeyron relation [Eq. (5)], we obtain the desired fluctuation-dissipation theorem

$$\langle \xi_{\mathbf{k}} \xi_{-\mathbf{k}} \rangle = \frac{m_E}{(1 - K_E) \Gamma k^2} = \frac{k_B T_E}{\gamma k^2}, \quad (33)$$

which establishes the consistency of the Langevin formalism. Implicit in this result is the fact that bulk forces—with correlations identical to those present when each phase is treated as an infinite system—suffice to generate the correct equilibrium interfacial fluctuations when

$$\langle \xi_{\mathbf{k}} \xi_{-\mathbf{k}} \rangle = \frac{m_E}{(1 - K_E) \Gamma k^2} \int_{-\infty}^{+\infty} \frac{d\Omega}{\pi} \text{Re} \left[\frac{1}{g(\Omega)} \right], \quad (31)$$

where

both phases are present. Effectively, this implies that the interface has no net effect on these forces.

III. INTERFACE FORCE

In this section we examine the effect of the interface force on interfacial fluctuations. For simplicity, we consider the symmetric model of a pure substance where both phases are assumed to have the same thermodynamic properties (the issues associated with having different phases having been resolved above). This model is defined by Eqs. (17), (18), and (21) with $C_L = 0$. For shortness of notation we define $D_T = D_S^T = D_L^T$ and $c = c_L = c_S$. Once linearized about a planar interface, the integral equation for this model takes the form

$$\begin{aligned} & \Gamma \nabla_{\perp}^2 \xi(\mathbf{r}, t) - \frac{1}{\mu} \frac{\partial \xi(\mathbf{r}, t)}{\partial t} + \eta(\mathbf{r}, t) \\ &= \int_{-\infty}^t \frac{dt'}{[4\pi D_T(t-t')]^{3/2}} \left\{ \int d^2 r' \exp\left(-\frac{|\mathbf{r}-\mathbf{r}'|^2}{4D_T(t-t')}\right) \left[\frac{L}{c} \frac{\partial \xi(\mathbf{r}', t')}{\partial t'} + q_z^S(\mathbf{p}) - q_z^L(\mathbf{p}) \right] \right. \\ & \quad \left. - \int d^2 r' \exp\left(-\frac{|\mathbf{r}-\mathbf{r}'|^2 + z'^2}{4D_T(t-t')}\right) \left[\int_{-\infty}^0 dz' \nabla' \cdot \mathbf{q}^S(\mathbf{R}', t') + \int_0^{\infty} dz' \nabla' \cdot \mathbf{q}^L(\mathbf{R}', t') \right] \right\}. \end{aligned} \quad (34)$$

We note that although in the symmetric case the bulk forces of each phase have the same variance, instantaneous fluctuations on each side of the interface $\mathbf{q}^v(\mathbf{p})$ need not be the same, as in the nonsymmetric case, and need to be kept separate. The contributions of the interface terms $\mathbf{q}^v(\mathbf{p})$ originating from the heat conservation condition [Eq. (18)] are canceled exactly by the two boundary terms resulting from integrating by parts over dz' the volume integrals containing the divergences of the bulk forces.

Next, we evaluate $\langle \xi_{\mathbf{k}\omega} \xi_{\mathbf{k}'\omega'} \rangle$ by Fourier transforming the above equation following steps identical to those detailed in Appendix A for the two-sided model. After lengthy manipulations we obtain

$$\langle \xi_{\mathbf{k}\omega} \xi_{\mathbf{k}'\omega'} \rangle = [\langle \eta_{\mathbf{k}\omega} \eta_{\mathbf{k}'\omega'} \rangle + \langle B_{\mathbf{k}\omega} B_{\mathbf{k}'\omega'} \rangle] / [S_{\mathbf{k}\omega} S_{\mathbf{k}'\omega'}], \quad (35)$$

where

$$\langle \eta_{\mathbf{k}\omega} \eta_{\mathbf{k}'\omega'} \rangle = 2 \frac{k_B T_M^2}{\mu L} (2\pi)^3 \delta(\mathbf{k} + \mathbf{k}') \delta(\omega + \omega'), \quad (36)$$

$$\begin{aligned} \langle B_{\mathbf{k}\omega} B_{\mathbf{k}'\omega'} \rangle &= 2 \frac{D_T k_B T_M^2}{c} \frac{(2\pi)^3 \delta(\mathbf{k} + \mathbf{k}') \delta(\omega + \omega')}{4 D_T^2 \text{Re}[Z_{\mathbf{k}\omega}^{1/2}]} \\ & \times \left(1 + \frac{\text{Re}[Z_{\mathbf{k}\omega}]}{(Z_{\mathbf{k}\omega} Z_{\mathbf{k}'\omega'})^{1/2}} \right), \end{aligned} \quad (37)$$

$$S_{\mathbf{k}\omega} = \frac{L i \omega}{2 c D_T Z_{\mathbf{k}\omega}^{1/2}} + \Gamma k^2 + i\omega/\mu, \quad (38)$$

$$Z_{\mathbf{k}\omega} = k^2 + i\omega/D_T, \quad (39)$$

and Re denotes the real part.

To isolate the separate contributions of the bulk and interface forces, we express the static spectrum in the form

$$\langle \xi_{\mathbf{k}} \xi_{-\mathbf{k}} \rangle = \frac{k_B T_M}{\gamma k^2} [F_B(d_0 k; \bar{\mu}) + F_I(d_0 k; \bar{\mu})], \quad (40)$$

where

$$\left(\frac{F_B(d_0 k; \bar{\mu})}{F_I(d_0 k; \bar{\mu})} \right) = \frac{\gamma k^2}{(2\pi)^4 k_B T_M} \int d\omega d\omega' d^2 k' \times \left(\frac{\langle B_{\mathbf{k}\omega} B_{\mathbf{k}'\omega'} \rangle / [S_{\mathbf{k}\omega} S_{\mathbf{k}'\omega'}]}{\langle \eta_{\mathbf{k}\omega} \eta_{\mathbf{k}'\omega'} \rangle / [S_{\mathbf{k}\omega} S_{\mathbf{k}'\omega'}]} \right) \quad (41)$$

give the contribution of each noise source, $d_0 = \Gamma c/L$ is the usual capillary length, and we have defined the dimensionless kinetic coefficient:

$$\bar{\mu} = \frac{\mu \Gamma}{D_T}. \quad (42)$$

With this choice of definition $(k_B T_M / \gamma k^2) F_B(d_0 k; \bar{\mu})$ gives exactly the interfacial fluctuation spectrum that would be obtained with only the bulk force, and $(k_B T_M / \gamma k^2) F_I(d_0 k; \bar{\mu})$, the spectrum obtained with only the interface force.

Finally, by making the change of variable $\Omega = \omega / (D_T k^2)$, using Eqs. (36)–(39) and further manipulations we can express the functions $F_B(d_0 k; \bar{\mu})$ and $F_I(d_0 k; \bar{\mu})$ in the form

$$F_B(d_0 k; \bar{\mu}) = \int_{-\infty}^{+\infty} \frac{d\Omega}{\pi} \frac{1}{h(\Omega)} \text{Re}[1/g(\Omega)], \quad (43)$$

$$F_I(d_0 k; \bar{\mu}) = \frac{2d_0 k}{\bar{\mu}} \int_{-\infty}^{+\infty} \frac{d\Omega}{\pi} \frac{1}{h(\Omega)} \frac{\text{Re}[1/g(\Omega)]}{\text{Re}[1/(1+i\Omega)^{1/2}]}, \quad (44)$$

with the definitions

$$g(\Omega) = 2d_0 k (1 + i\Omega/\bar{\mu}) (1 + i\Omega)^{1/2} + i\Omega, \quad (45)$$

$$h(\Omega) = 1 - \left[(1 + \Omega^2)^{1/2} - 1 \right] / \bar{\mu}. \quad (46)$$

There are several properties of the functions $F_B(d_0 k; \bar{\mu})$ and $(F_I d_0 k; \bar{\mu})$ of relevance here. These can be derived by a combination of residue integrals in the complex Ω plane and numerical integration. The details of those calculations need not be reported here and we only quote the results. As a useful guide, we have plotted in Fig. 1 $F_B(d_0 k; \bar{\mu})$ and $F_I(d_0 k; \bar{\mu})$ as a function of $d_0 k$ for a typical value $\bar{\mu} = 5 \times 10^{-3}$. Note that the present result are only valid for $d_0 k \ll 1$ (when $d_0 \sim k$, the fluctuation scale becomes comparable to the interface thickness at which point the hydrodynamic description breaks down).

The first property is given by the relation

$$F_B(d_0 k; \bar{\mu}) + F_I(d_0 k; \bar{\mu}) = 1 \quad (47)$$

valid for all values of $d_0 k$ and $\bar{\mu}$. Combined with Eq. (40), it is directly seen to be an independent verification of the consistency of the Langevin formalism with equilibrium fluctuations.

The other properties, of direct interest here, determine the crossover between the two regimes dominated respectively by the bulk and the interface force. They can be expressed in the form

$$F_B(d_0 k, \bar{\mu}) \cong 1, \quad (48)$$

$$F_I(d_0 k, \bar{\mu}) \cong 0,$$

for $k \ll k^*$

$$F_B(d_0 k, \bar{\mu}) \cong 0, \quad (49)$$

$$F_I(d_0 k, \bar{\mu}) \cong 1,$$

for $k \gg k^*$, and

$$F_B(d_0 k^*, \bar{\mu}) \cong F_I(d_0 k^*, \bar{\mu}) \cong \frac{1}{2}, \quad \bar{\mu} \ll 1 \quad (50)$$

where the crossover scale $\lambda^* \equiv 2\pi/k^*$ is given by

$$\lambda^* \cong \frac{4\pi d_0}{\bar{\mu}} = \frac{4\pi c D_T}{\mu L}. \quad (51)$$

Interfacial fluctuations of wavelength λ^* (corresponding to the intersection of the two curves in Fig. 1) are affected equally by both forces while those on scales larger (smaller) than λ^* are affected only by the bulk (interface) force.

The physical origin of the crossover scale λ^* can be understood by noting that, following some perturbation, the interface relaxes by the effect of surface tension which, itself, acts via two different processes: (i) diffusion of heat in the bulk phases and (ii) interfacial kinetics. The relaxation rates of these two processes are given, respectively, by the poles of $S_{\mathbf{k}\omega}$ in the limit $\mu \rightarrow \infty$ and $D_T \rightarrow \infty$:

$$\omega_B \cong -i \frac{2c D_T \Gamma}{L} k^3, \quad (52)$$

$$\omega_I \cong -i \mu \Gamma k^2. \quad (53)$$

As k increases, ω_B increases as k^3 faster than ω_I which increases as k^2 . Therefore there exist a crossover scale, determined by $\omega_B \sim \omega_I$, at which the two processes have exactly the same decay rate. This relation yields at once $1/k^* \sim 2d_0/\bar{\mu}$ which concurs with Eq. (51). On scales much larger than λ^* , perturbations associated with interface force relax much faster than those associated with bulk force (i.e., $\omega_I \gg \omega_B$). Hence interfacial fluctuations are dominated by the latter. On the contrary, on scales much smaller than λ^* these perturbations relax much slower than those associated with the bulk force (i.e., $\omega_I \ll \omega_B$) and, hence, interfacial fluctuations are dominated by the interface force.

A. Physical relevance

In principle, to study the effect of the interface force on sidebranching we should perform a detailed calculation of noise amplification analogous to that of Ref. [5]. However, without embarking in such a calculation, a crude order of magnitude estimate of the growth rate at which this force becomes relevant can be obtained by comparing λ^* to the usual stability length of the planar interface

$$\lambda_S \sim \sqrt{\frac{d_0 D_T}{v}}. \quad (54)$$

The interface is stable on scales shorter than λ_S , such that only fluctuations on scales larger than λ_S become amplified by morphological instabilities. In dendritic growth where the interface is nonplanar, λ_S provides a relatively good estimate of the scale above which fluctuations are amplified. It is therefore reasonable to assume that the interface force should become relevant when the stability length becomes shorter than λ^* . When this occurs, part of the band of wave vector which becomes selectively amplified by morphological instabilities is strongly affected by the interface force (cf. Fig. 1). Since λ_S decreases with velocity, this crossover will occur when the velocity exceeds the value $v^* \sim \bar{\mu}^2 D_T / d_0$ obtained by setting $\lambda_S \sim \lambda^*$. In terms of physical parameters, this velocity takes the form

$$v^* \sim \frac{\mu^2 \gamma T_M}{c D_T}. \quad (55)$$

It should be remarked that to determine v^* we have implicitly assumed that we can use the equilibrium spectrum, in particular the expression for the crossover scale λ^* , to infer when fluctuations *outside of equilibrium* are affected by the interface force. This assumption should be valid at low velocity—in which case the fluctuation spectrum of the moving interface on scales shorter than λ_S can easily be seen (by performing a calculation analogous to that of Sec. IVB for pure materials) to be close to the equilibrium one—but should start to break down when the diffusion length D_T/v becomes significantly shorter than λ_S . However, for pure materials, the velocity at which this occurs is much larger than the values of v^* estimated below. We therefore expect Eq. (55) to provide a relatively good estimate for these materials.

For monatomic metals (Al, Cu, Ni, etc.), a good order of magnitude estimate of the kinetic coefficients μ , consistent with a large body of rapid solidification experiments, is given by the expression [24]

$$\mu = \frac{V_S L}{R T_M^2}, \quad (56)$$

where V_S is the speed of sound in the bulk (on the order of 2000 m/sec), L is the latent heat per mole, and R is the molar gas constant. This relation yields large values of μ on the order of a few m/sec K. This in turn yields values of $\bar{\mu}$ in the range 10^{-3} – 10^{-2} , λ^* in the range of a few hundred nm to 1 μm , and values of v^* in the range of several cm/sec to a few m/sec.

For transparent organic materials with large molecules (SCN, pivalic acid, etc.), the value of μ is not precisely known, but is believed to be much smaller and fall within the range 10^{-3} – 10^{-1} m/sec K. For $\mu = 10^{-2}$ m/sec K and

material parameters corresponding to SCN, $\bar{\mu} \cong 6 \times 10^{-3}$, $\lambda^* \cong 7 \mu\text{m}$, and $v^* \cong 1.5$ mm/sec, while, for $\mu = 10^{-3}$ m/sec K, $v^* \cong 15 \mu\text{m}/\text{sec}$. Although firm conclusions cannot be drawn without precise measurements of μ , these estimates suggest that the effect of the interface force may become relevant at much smaller velocities for this class of materials.

IV. NONEQUILIBRIUM STEADY STATES

A. Fluctuations about a stationary planar interface in a temperature gradient

We first examine the fluctuations of a stationary interface in a temperature gradient. We present an exact calculation of this spectrum for the symmetric model of a pure substance and then discuss its extension to binary alloys. As we shall see, part of this spectrum can be recovered more directly using fluctuation theory. This alternate derivation provides additional physical insight and is included at the end.

The equations of interest are given by Eqs. (17) and (18) together with the interface boundary condition

$$T_I = T_M - G \xi - \Gamma \kappa. \quad (57)$$

The Langevin formalism is extended outside of equilibrium by making the usual assumption that the magnitude of the bulk force is determined by the local value of the temperature:

$$\langle q_i(\mathbf{R}, t) q_j(\mathbf{R}', t') \rangle_G = \frac{2 D_T k_B T_{SS}(\mathbf{R})^2}{c} \times \delta(\mathbf{R} - \mathbf{R}') \delta(t - t') \delta_{ij}, \quad (58)$$

where $T_{SS}(\mathbf{R})$ is the steady-state temperature profile

$$T_{SS}(\mathbf{R}) = T_M + G z. \quad (59)$$

We introduce the subscript G on all averages to distinguish them from the equilibrium averages of Sec. II. The fact that the magnitude of the force varies spatially via the steady-state profile complicates tremendously the calculation of the nonequilibrium bulk fluctuations [25]. This is due to the fact that the Fourier transform of Eq. (58) in the z direction couples different modes. However, in the present situation, we are interested in calculating fluctuations about an interface which is perpendicular to the z axis. Equation (58) can then be Fourier transformed in \mathbf{r} and the z dependence of the magnitude of the force can be integrated out exactly via the projection of the force onto the interface.

The analog of Eq. (34) is given by

$$\begin{aligned} & \Gamma \nabla_{\perp}^2 \xi(\mathbf{r}, t) - G \xi(\mathbf{r}, t) \\ &= \int_{-\infty}^t \frac{dt'}{[4\pi D_T(t-t')]^{3/2}} \\ & \times \left\{ \int d^2 r' \exp\left(-\frac{|\mathbf{r}-\mathbf{r}'|^2}{4D_T(t-t')}\right) \left[\frac{L}{c} \frac{\partial \xi(\mathbf{r}', t')}{\partial t'} + q_z^S(\mathbf{p}) - q_z^L(\mathbf{p}) \right] \right. \\ & \left. - \int d^2 r' \exp\left(-\frac{|\mathbf{r}-\mathbf{r}'|^2 + z'^2}{4D_T(t-t')}\right) \left[\int_{-\infty}^0 dz' \nabla' \cdot \mathbf{q}^S(\mathbf{R}', t') + \int_0^{\infty} dz' \nabla' \cdot \mathbf{q}^L(\mathbf{R}', t') \right] \right\}. \quad (60) \end{aligned}$$

The temperature gradient enters in the problem in two distinct ways: (i) via the interface boundary condition [$G\xi$ term in Eq. (60)], and (ii) via the projection of the bulk force on the interface. The first damps out intermediate scale fluctuations while the second enhances large scale fluctuations. The physical origin of this enhancement is directly related to the fact that the strength of the noise is proportional to the square of $T_{SS}(\mathbf{R})$. This implies that the projection of the temperature fluctuations on the hotter liquid side outweighs that of fluctuations on the colder solid side. If the noise strength was linear in temperature, this effect would be completely absent.

To calculate the fluctuation spectrum we again Fourier transform Eq. (60) following steps identical to those outlined in Appendix A. To see where the large scale fluctuation enhancement originates from, we write down the intermediate result

$$\langle B_{\mathbf{k}\omega} B_{\mathbf{k}'\omega'} \rangle_G = \frac{(2\pi)^3 \delta(\mathbf{k} + \mathbf{k}') \delta(\omega + \omega')}{4 D_T^2 (Z_{\mathbf{k}\omega} Z_{\mathbf{k}'\omega'})^{1/2}} \int_{-\infty}^{+\infty} dz \exp \left[-(Z_{\mathbf{k}\omega}^{1/2} + Z_{\mathbf{k}'\omega'}^{1/2}) |z| \right] \left[k^2 + (Z_{\mathbf{k}\omega} Z_{\mathbf{k}'\omega'})^{1/2} \right] F(z), \quad (61)$$

where

$$F(z) = \frac{2D_T k_B T_M^2}{c} \left[1 + 2 \frac{Gz}{T_M} + \left(\frac{Gz}{T_M} \right)^2 \right] \quad (62)$$

and $\langle \xi_{\mathbf{k}\omega} \xi_{\mathbf{k}'\omega'} \rangle_G = \langle B_{\mathbf{k}\omega} B_{\mathbf{k}'\omega'} \rangle_G / S_{\mathbf{k}\omega} S_{\mathbf{k}'\omega'}$ with

$$S_{\mathbf{k}\omega} = \frac{L i \omega}{2 c D_T Z_{\mathbf{k}\omega}^{1/2}} + \Gamma k^2 + G. \quad (63)$$

The term proportional to Gz/T_M in $F(z)$ is odd and gives a vanishing contribution once integrated in Eq. (61). The term proportional to $(Gz/T_M)^2$ gives a finite contribution which corresponds precisely to the aforementioned fluctuation enhancement. This enhancement only affects long-wavelength fluctuations since the diffusion kernel decays approximately as $\exp(-2k|z|)$ at small k . Hence the contribution of the term proportional to $(Gz/T_M)^2$ only becomes significant when $k \sim G/T_M$. After integrating Eq. (61) over z we obtain

$$\langle B_{\mathbf{k}\omega} B_{\mathbf{k}'\omega'} \rangle_G = \langle B_{\mathbf{k}\omega} B_{\mathbf{k}'\omega'} \rangle \left[1 + \left(\frac{G}{T_M} \right)^2 \frac{1}{k^2 + (Z_{\mathbf{k}\omega} Z_{\mathbf{k}'\omega'})^{1/2}} \right], \quad (64)$$

where $\langle B_{\mathbf{k}\omega} B_{\mathbf{k}'\omega'} \rangle$ is the equilibrium value given by Eq. (37). Finally, using Eq. (30) and making the change of variable $\Omega = \omega / (D_T k^2)$ we obtain

$$\langle \xi_{\mathbf{k}\omega} \xi_{-\mathbf{k}} \rangle_G = \frac{k_B T_M}{\gamma (k^2 + a^{-2})} \int_{-\infty}^{+\infty} \frac{d\Omega}{\pi} \text{Re} \left[\frac{1}{g(\Omega)} \right] \times \left[1 + \frac{(kb)^{-2}}{1 + (1 + \Omega^2)^{1/2}} \right], \quad (65)$$

with the definition

$$g(\Omega) = \frac{2d_0(k^2 + a^{-2})}{k} (1 + i\Omega)^{1/2} + i\Omega \quad (66)$$

and the two crossover length scales

$$a = \left(\frac{\gamma T_M}{L G} \right)^{1/2}, \quad (67)$$

$$b = \frac{T_M}{G}. \quad (68)$$

Although b decreases with G faster than a , it is always several orders of magnitude larger since the ratio γ/L

in Eq. (67) is a microscopic length $\sim d_0$. The form of the spectrum on scales smaller and larger than b can be calculated directly from Eq. (65). The two limits of interest take the form

$$\langle \xi_{\mathbf{k}} \xi_{-\mathbf{k}} \rangle_G \cong \frac{k_B T_M}{\gamma} \frac{1}{k^2 + a^{-2}}, \quad kb \gg 1 \quad (69)$$

$$\langle \xi_{\mathbf{k}} \xi_{-\mathbf{k}} \rangle_G \cong \frac{k_B}{2c} \frac{1}{k}, \quad kb \ll 1 \quad (70)$$

or, in real space,

$$\langle \xi(\mathbf{r}) \xi(\mathbf{r}') \rangle_G \sim \frac{k_B T_M}{\gamma} K_0(|\mathbf{r} - \mathbf{r}'|/a) \quad \text{for } |\mathbf{r} - \mathbf{r}'| \ll b \quad (71)$$

$$\langle \xi(\mathbf{r}) \xi(\mathbf{r}') \rangle_G \sim \frac{k_B}{c} \frac{1}{|\mathbf{r} - \mathbf{r}'|} \quad \text{for } |\mathbf{r} - \mathbf{r}'| \gg b, \quad (72)$$

where K_0 denotes the zeroth order modified Bessel function. The temperature gradient therefore screens the logarithmically diverging equilibrium correlations on intermediate scales and induces long-range correlations on very large scales induced by the projection of bulk temperature fluctuations onto the interface. As an illustration, a plot of the complete spectrum is shown in Fig. 2.

For binary alloys, results are identical to those of Eqs. (69) and (70) with the only difference that the melting temperature T_M should be replaced by the equilibrium temperature $T_E = T_M - m_E C_L^0$; in particular, the two crossover lengths become $a = (\gamma T_E / LG)^{1/2}$ and $b = T_E / G$. Also, a calculation of the spectrum of the one-sided model yields the result

$$\langle \xi_{\mathbf{k}} \xi_{-\mathbf{k}} \rangle_G = \frac{m_E}{(1 - K_E)(G + \Gamma k^2)} \quad (73)$$

which, together with the Clausius-Clapeyron relation [Eq. (5)], reduces exactly to Eq. (69). This model only misses the long-wavelength part of the complete spectrum [Eq. (70)] since it does not include temperature fluctuations.

Fluctuation theory revisited

There is a more direct way to derive the result of Eq. (69) which does not require using the Langevin formalism and applies equally to pure materials and binary al-

loys. It is based on the observation that, on scales much smaller than b , the entire two-phase system can be considered to be in local thermodynamic equilibrium with respect to the temperature gradient, in which case fluctuation theory can be applied. The role of the temperature gradient, on these scales, becomes completely analogous to that of gravity on a liquid-gas system. The only “truly nonequilibrium” effect of the gradient is via the aforementioned fluctuation enhancement on scales larger than b which is not describable by fluctuation theory.

In the presence of a temperature gradient, the minimum work W necessary to carry out reversibly a fluctuation of the interface has an additional contribution associated with the work of the pressure forces. The difference of pressure across the interface $P_L - P_S$ is no longer zero but varies with z as

$$P_L - P_S = \left[\left(\frac{\partial P_L}{\partial T} \right)_{\mu_L} - \left(\frac{\partial P_S}{\partial T} \right)_{\mu_S} \right] G z = \frac{L}{T_E} G z . \quad (74)$$

The analog of Eq. (10) becomes

$$W = \int_0^{\delta V_S} (P_L - P_S) dV_S + \gamma \delta A , \quad (75)$$

where we have used the total volume conservation condition $dV_L = -dV_S$, and δV_S denotes the total volume change during the fluctuation.

Combining Eqs. (74) and (75) we obtain at once

$$W[\xi] = \int d^2 r \left(\frac{L G}{T_E} \int_0^{\xi(\mathbf{r})} z dz + \frac{\gamma}{2} |\nabla_{\perp} \xi(\mathbf{r})|^2 \right) . \quad (76)$$

After performing the integration over z , the probability distribution of Gaussian fluctuations becomes

$$p = \frac{1}{Z} \exp \left[-\frac{1}{k_B T_E} \int d^2 r \left(\frac{L G}{T_E} \frac{1}{2} \xi(\mathbf{r})^2 + \frac{\gamma}{2} |\nabla_{\perp} \xi(\mathbf{r})|^2 \right) \right] . \quad (77)$$

This distribution yields at once the spectrum of Eq. (69). In a liquid-gas system [32] the probability distribution of interfacial fluctuations is identical to Eq. (77) with the substitution $L G/T_E \rightarrow (\rho_L - \rho_G)g$ (g being the acceleration of gravity and ρ the mass density).

B. Fluctuations about a moving planar interface

1. Basic equations

We now extend the calculations of Sec. IV A to a situation where the interface is constrained to move at some constant velocity v . Since we are primarily interested in binary alloys, we restrict our attention to the usual one-sided model of directional solidification [19]. The basic equations in the frame moving at velocity v with the in-

terface are given by

$$\frac{\partial C_L}{\partial t} = v \frac{\partial C_L}{\partial z} + D_L \Delta C_L - \nabla \cdot \mathbf{q}^L(\mathbf{R}, t) , \quad (78)$$

$$C_L(1 - K_E)v_n = -\hat{\mathbf{n}} \cdot D_L \nabla C_L + \hat{\mathbf{n}} \cdot \mathbf{q}^L(\mathbf{p}) , \quad (79)$$

$$\frac{C_L - C_L^0}{\Delta C^0} = -\frac{\xi}{l_T} - d_0^c \kappa , \quad (80)$$

where the magnitude of the force is determined by the local concentration

$$\langle q_i^L(\mathbf{R}, t) q_j^L(\mathbf{R}', t') \rangle_v = 2 D_L C_{SS}(\mathbf{R}) \delta(\mathbf{R} - \mathbf{R}') \times \delta(t - t') \delta_{ij} \quad (81)$$

and $C_{SS}(\mathbf{R})$ represents the steady-state profile of the planar interface

$$C_{SS}(\mathbf{R}) = C_{\infty}(1/K_E - 1) \exp(-v z/D_L) + C_{\infty} . \quad (82)$$

The three basic length scales of the model are the thermal length l_T , the chemical capillary length d_0^c , and the diffusion length l defined by

$$\begin{aligned} l_T &= (m_E \Delta C^0)/G , \\ d_0^c &= \Gamma/(m_E \Delta C^0) , \\ l &= 2 D_L/v , \end{aligned} \quad (83)$$

where $\Delta C^0 = C_{\infty}(1/K_E - 1)$ is the miscibility gap of the steady-state planar interface and C_{∞} is the nominal composition of the alloy. The crossover scales a and b expressed in terms of l_T and d_0^c take the form

$$a = (d_0^c l_T)^{1/2} , \quad (84)$$

$$b = (T_E/m_E \Delta C^0) l_T ,$$

where T_E now denotes the temperature of the planar interface given by

$$T_E = T_M - m_E \frac{C_{\infty}}{K_E} . \quad (85)$$

It is also customary [19] to define the dimensionless control parameters

$$\nu = 2l_T/l , \quad (86)$$

$$V = d_0^c/l ,$$

in terms of which the growth rate $\omega(k; v)$ of sinusoidal perturbations of the planar interface resulting from the usual Mullins-Sekerka analysis [21] can be written in the form

$$\frac{\omega(k; v) l^2}{2 D_L} = A(kl) \left[1 - \frac{1}{\nu} - \frac{V}{2} (kl)^2 \right] - 2 K_E , \quad (87)$$

where

$$A(kl) = \sqrt{1 + (kl)^2} - 1 + 2 K_E .$$

[Note that the above result is the growth rate obtained by neglecting the term $\partial C_L/\partial t$ in Eq. (78) which is accurate at small growth rate.] In the limit $V \ll 1$, the onset velocity v_c and the critical wave number k_c are determined respectively by the relations

$$\nu_c \cong 1 + 3(K_E^2 V_c/2)^{1/3}, \quad (88)$$

$$k_c l \cong (2K_E/V_c)^{1/3}, \quad (89)$$

where $\nu_c \equiv l_T v_c/D_L$ and $V_c \equiv d_0^c v_c/2D_L$.

As emphasized in Sec. III, using the one-sided model neglects the effect of temperature fluctuations and, thus, the enhancement of interfacial fluctuation on scales larger than b . The question then arises as to whether it is safe to neglect this enhancement. Here, we are mainly interested in capturing the correct interfacial fluctuations over the range of scale where these fluctuations become amplified by morphological instabilities beyond the onset velocity v_c . This question can therefore be answered by determining where b^{-1} lies in comparison to the minimum unstable wave vector above onset. Very near onset, the latter scales as $k_{\min} \sim (d_0^c l_T^2)^{-1/3}$, which is always much larger than b^{-1} , and, further away from onset,

$$k_{\min} = \left(\frac{\nu}{\nu-1} \right) \frac{K_E}{l_T} \quad (90)$$

$$S_{\mathbf{q}\Omega} = \frac{1}{\nu} - 1 + \frac{V}{2} q^2 + \frac{1 + i\Omega - (1 - 2K_E)(1/\nu + Vq^2/2)}{Y_{\mathbf{q}\Omega}^{1/2}}, \quad (95)$$

$$Y_{\mathbf{q}\Omega} = q^2 + 2i\Omega + 1, \quad (96)$$

$$N(\Omega, q) = \frac{(q^2 + |Y_{\mathbf{q}\Omega}| - 2 \operatorname{Re}[Y_{\mathbf{q}\Omega}^{1/2}] + 1) (\operatorname{Re}[Y_{\mathbf{q}\Omega}^{1/2}] - 1 + K_E)}{|Y_{\mathbf{q}\Omega}| (1 - K_E) (\operatorname{Re}[Y_{\mathbf{q}\Omega}^{1/2}] - 1) \operatorname{Re}[Y_{\mathbf{q}\Omega}^{1/2}]}. \quad (97)$$

The zero of $S_{\mathbf{q}\Omega}$ with $\Omega = 2D_L \omega/v^2$ determines the decay rate of perturbations of the planar interface [in the quasistationary limit where $Y_{\mathbf{q}\Omega} = q^2 + 1$ this rate reduces to the form of Eq. (87)]. There are two interesting limits of this spectrum which can be extracted analytically. The first takes the form

$$C(k; v \rightarrow 0) \cong \frac{k_B T_E}{\gamma} \frac{1}{k^2 + a^{-2}} \quad (98)$$

and is essentially the consistency relation that, in the limit of very small velocity [i.e., $l \rightarrow \infty$ in terms of Eq. (93)], the spectrum reduces to that of the stationary interface given by Eq. (69). The second takes the form

$$C(k_c; v) \cong \frac{k_B T_E a^2}{\gamma} \frac{c_1}{1 - v/v_c} \quad \text{for } 1 - v/v_c \ll 1 \quad (99)$$

and exhibits the usual divergence of the amplitude of fluctuations slightly below the onset of instability. Here, c_1 is a constant of order unity whose value can be extracted analytically by examining the behavior of the function

for $\nu - 1 \gg V_c$. Since $\nu/(\nu - 1)$ is always of order unity, the condition that k_{\min} becomes much smaller than b^{-1} becomes

$$\frac{(1 - K_E)m_E C_\infty}{T_E K_E^2} \gg 1. \quad (91)$$

2. Interfacial fluctuations

We define the fluctuation spectrum of a moving interface by

$$C(k; v) \equiv \langle \xi_{\mathbf{k}} \xi_{-\mathbf{k}} \rangle_v. \quad (92)$$

To calculate this spectrum we start from the boundary integral formulation of the one-sided model and solve the resulting linear integral equation for $\xi(\mathbf{r}, t)$ by Fourier transform. The calculations are presented in Appendix B and the final result can be expressed in the form

$$C(k; v) = \frac{k_B T_E a^2}{\gamma} f(kl; V, \nu), \quad (93)$$

where

$$f(q; V, \nu) = \frac{1 - K_E}{2\nu} \int_{-\infty}^{+\infty} \frac{d\Omega}{\pi} \frac{N(\Omega, q)}{|S_{\mathbf{q}\Omega}|^2} \quad (94)$$

and

$f(kl; V, \nu)$ as $v \rightarrow v_c$. In the limit $V_c \ll 1$, c_1 is equal to unity.

To illustrate the enhancement of fluctuations below onset, we have evaluated the integral over Ω numerically and plotted the spectrum in Fig. 3 for several values of $v/v_c = 0, 0.5, 0.8, 0.9, 0.99$, and parameters corresponding to a succinonitrile-0.10 wt % acetone alloy with $G = 38.2$ K/cm. The onset of morphological instability for this particular alloy and growth condition has been studied experimentally by Eshelman and Trivedi [26]. The necessary material constants are given by $L/c = 23$ K, $\Gamma = 0.64 \times 10^{-7}$ K m, $m_E = 2.8$ K/wt %, and $K_E = 0.1$. For this value of G , these yield $v_c = 1.97$ $\mu\text{m}/\text{sec}$, $V_c = 1.92 \times 10^{-5}$, $\nu_c = 1.0137$, $d_0 = 2.8 \times 10^{-9}$ m, $d_0^c = 2.53 \times 10^{-8}$ m, and $d_0 k_c = 4.6 \times 10^{-5}$. We have purposely used the dimensionless combination $d_0 k$ to allow a comparison of Fig. 2 and Fig. 3. The fluctuation enhancement below onset falls on the right-hand portion of this plateau, far from the small k enhancement due to bulk temperature fluctuations. Also, note that the magnitude of the maxima of the spectra for different v remain well described by Eq. (99), even beyond

its range of strict validity [$\max\{C(k;v)\} \cong 1, 2, 5, 10, 100$ for $v/v_c = 0, 0.5, 0.8, 0.9, 0.99$].

V. NOISE AMPLIFICATION NEAR ONSET

We consider the situation where the pulling speed of the sample in a directional solidification experiment is changed abruptly from an initial value $v_0 < v_c$ to some value $v_1 > v_c$:

$$v_p(t) = \begin{cases} v_0 < v_c & \text{for } t < 0 \\ v_1 > v_c & \text{for } t > 0. \end{cases} \quad (100)$$

There are two essential time scales. The first is the solutal diffusion time $\tau_D = 2D_L/v_1^2$ mentioned in the Introduction. It fixes the duration of the dynamical transient (typically several τ_D) during which the interface adjusts its boundary layer of solute and, hence, its velocity, to the new pulling speed v_1 . A detailed study of this transient and a comparison to the WL boundary-layer analysis is given in Ref. [33]. The second, $\tau_1 = 1/\omega(k_c; v_1)$, fixes the time scale over which fluctuations become amplified. In the generic case of metallurgical relevance $v_0 = 0$ and v_1 is significantly larger than v_c . In this case, τ_1 is comparable to or smaller than τ_D which, in turn, imply that the interface becomes unstable during its transient response to the change of pulling speed.

Here, we consider the opposite limit where both v_0 and v_1 are close to v_c and, in addition, $\tau_D \cong 2D_L/v_c^2 \ll \tau_1$. The latter condition is additional since v_1 being close to v_c does not necessarily imply that $\tau_D \ll \tau_1$. In this limit, the interface relaxes to its new velocity v_1 before fluctuations are significantly amplified, which allows us to neglect the dynamical transient of the interface. It should be noted that there is a second critical velocity v'_c (commonly referred to as the absolute stability limit) beyond which the interface is again restabilized. For typical alloy composition, this velocity is very large (in the cm/sec to m/sec range), and not accessible by the standard Bridgman directional solidification technique, except for extremely dilute alloys where v'_c (in the 100 $\mu\text{m}/\text{sec}$ to mm/sec range) becomes accessible. Although our analytical treatment will be presented within the context of the lower limit v_c , the expressions that are derived also apply to the upper limit with the simple substitution $v_c \rightarrow v'_c$ and the subscript, of v_0 and v_1 interchanged.

A. Theory

Formally, the interface position can be written in the form

$$h(\mathbf{r}, t) = h_0(t) + \xi(\mathbf{r}, t), \quad (101)$$

where $h_0(t)$ represents the dynamical transient response of the planar interface whose velocity is simply $v(t) = dh_0/dt$. As before, $\xi(\mathbf{r}, t)$ represents the linear response of the interface to fluctuations. The essence of the problem consists in calculating the time-dependent fluctuation spectrum

$$C(k; t) \equiv \langle \xi_{\mathbf{k}}(t) \xi_{-\mathbf{k}}(t) \rangle \quad (102)$$

from which the ‘‘observable’’ mean-square amplitude

$$\langle \xi(t)^2 \rangle = \int \frac{d^2k}{(2\pi)^2} C(k; t) \quad (103)$$

can be constructed. To calculate $C(k, t)$ we follow the same procedure as in Refs. [11, 28], which consists in writing down a stochastic evolution equation for each Fourier mode

$$\frac{d\xi_{\mathbf{k}}(t)}{dt} = \omega(k; v(t)) \xi_{\mathbf{k}}(t) + f(t), \quad (104)$$

and projecting the fluctuation spectrum at $t = 0$. The latter requires choosing the stochastic force $f(t)$ such that

$$C(k, t = 0) = C(k, v_0), \quad (105)$$

where $C(k, v_0)$ is given by Eq. (93) derived in Sec. IV. Equation (104) has an exact formal solution which together with the above constraint on $f(t)$ yields at once the solution

$$C(k, t) = 2C(k, v_0) |\omega(k, v_0)| \int_{-\infty}^t dt' \times \exp \left[2 \int_{t'}^t dt'' \omega(k; v(t'')) \right]. \quad (106)$$

Furthermore, the interface velocity satisfies the two limits $v(t) = v_0$ for $t < 0$, $v(t) = v_1$ for $t \gg \tau_D$. Since we are interested in the amplification of fluctuations on a time scale which is itself much larger than τ_D , we can make the approximation that $v(t) = v_1$ for $t > 0$ which corresponds to neglecting the effect of the transient on a time scale $\sim \tau_D$. Substituting these forms of $v(t)$ into Eq. (106) we obtain after simple integrations:

$$C(k, \bar{t}) = C(k; v_0) \left(1 + \frac{\bar{\omega}(k; v_0)}{\bar{\omega}(k; v_1)} \right) \exp[2\bar{\omega}(k; v_1) \bar{t}], \quad (107)$$

where we have defined the dimensionless amplification rate $\bar{\omega}(k; v) \equiv \omega(k; v_0)\tau_D$ and dimensionless time $\bar{t} \equiv t/\tau_D$. For v close to v_c , $\bar{\omega}(k; v)$ can be expanded in the form

$$\bar{\omega}(k; v) \cong \bar{\omega}(k_c; v) - \frac{c_3}{2} \left(\frac{k - k_c}{k_c} \right)^2, \quad (108)$$

with

$$\bar{\omega}(k_c; v) \cong c_2 (1 - v_c/v) \quad (109)$$

and the constants c_2 and c_3 generally defined by Eq. (87); for $V_c \ll 1$, they take the simple form $c_1 \cong 1$, $c_2 \cong (2K_E/V_c)^{1/3}$, and $c_3 \cong 6K_E$.

The mean-square amplitude can then be obtained by noting that only wave vectors in the unstable band contribute significantly to the integral in Eq. (103) which can be rewritten in the form

$$\langle \xi(\bar{t})^2 \rangle = \int_{k_{\min} < k < k_{\max}} \frac{d^2k}{(2\pi)^2} C(k; \bar{t}), \quad (110)$$

where k_{\min} and k_{\max} are the two zeros of $\bar{\omega}(k; v_1)$. Combining Eqs. (107), (108), and (110) we obtain

$$\begin{aligned} \langle \xi(\bar{t})^2 \rangle &= \exp[2\bar{\omega}(k_c; v_1)\bar{t}] \int_{k_{\min} < k < k_{\max}} \frac{k dk}{2\pi} \\ &\times C(k; v_0) \left(1 + \frac{\bar{\omega}(k; v_0)}{\bar{\omega}(k; v_1)} \right) \\ &\times \exp\left(-c_3 \left[\frac{k - k_c}{k_c} \right]^2 \bar{t}\right). \end{aligned} \quad (111)$$

In the limit $\bar{t} \gg 1$, the integrand is sharply peaked around k_c and we can replace k by k_c everywhere except inside the factor of the exponential. We obtain at once

$$\begin{aligned} \langle \bar{\xi}(\bar{t})^2 \rangle &\cong C(k_c; v_0) \left(1 + \frac{\bar{\omega}(k_c; v_0)}{\bar{\omega}(k_c; v_1)} \right) \\ &\times \frac{\text{erf}\left[\sqrt{2\bar{\omega}(k_c; v_1)\bar{t}}\right] \exp[2\bar{\omega}(k_c; v_1)\bar{t}]}{\lambda_c^4 \sqrt{c_3\bar{t}/4\pi^3}}, \end{aligned} \quad (112)$$

where erf is the error function, $\lambda_c = 2\pi/k_c$ is the critical wavelength defined by Eq. (89), and we have defined the dimensionless mean-square amplitude

$$\langle \bar{\xi}(\bar{t})^2 \rangle \equiv \frac{\langle \xi(\bar{t})^2 \rangle}{\lambda_c^2}. \quad (113)$$

With the above definition, the crossover from the linear amplification regime to the nonlinear regime where fluctuations become observable occurs when $\langle \bar{\xi}(\bar{t})^2 \rangle$ is of order unity.

Finally, the above expression can be further simplified by eliminating $C(k_c; v_0)$ using Eq. (99), using the definition $a^2 = d_0^2 l_T$, and restricting our attention to times $\bar{t} \gg 1/c_2[1 - v_c/v_1]$. We obtain at once the final form:

$$\begin{aligned} \langle \bar{\xi}(\bar{t})^2 \rangle &\cong \frac{c_1 F}{\sqrt{c_3/4\pi^3}} \left(\frac{1}{1 - v_0/v_c} + \frac{1}{1 - v_c/v_1} \right) \\ &\times \frac{\exp(2c_2[1 - v_c/v_1]\bar{t})}{\sqrt{\bar{t}}}, \end{aligned} \quad (114)$$

where we have defined the small parameter

$$F = \frac{k_B T_E d_0 l_T}{\gamma \lambda_c^4}. \quad (115)$$

Also, our initial assumption that $\tau_D \ll \tau_1$ imposes the constraint on v_1

$$c_2 [1 - v_c/v_1] \ll 1. \quad (116)$$

B. Application to experiment

In principle, it should be possible to design a directional solidification experiment near onset to measure the magnitude of F directly using the result of Eq. (114). An easily observable quantity is the amplification time t_A at which the interface becomes deformed on a scale comparable to λ_c . Since F is very small, this time does not depend sensitively on the value of $\langle \bar{\xi}(\bar{t})^2 \rangle$ which together with the ratio $c_1/\sqrt{c_3/4\pi^3}$ can be approximated by unity. The amplification time then takes the simple form of Eq. (1) where c_2 is defined by Eqs. (87) and (109).

There are two main difficulties in performing such an experiment that would need to be overcome. The first is the constraint on v_1 imposed by Eq. (116). The second is the magnitude of the diffusion time τ_D . There is also the constraint $(1 - v_0/v_c) \ll 1$. However, this one can easily be met by choosing v_0 , for example, in the range $0.7 - 0.9v_c$. [Note that in Eq. (1) it would be necessary to use the experimentally determined value of v_c which can differ slightly from the theoretical one.] The constraint on v_1 is precisely the one that allows us to neglect the dynamical transient of the interface which follows the change of pulling speed. Using the small velocity expression for c_2 it can be expressed in the form

$$1 - v_c/v_1 \ll \left(\frac{\Gamma v_c}{m_E C_\infty [1 - K_E] D_L} \right)^{1/3}, \quad V_c \ll 1. \quad (117)$$

The practical difficulty of satisfying this constraint is related to the smallness of the ratio raised to the 1/3 power. This smallness in turn implies knowing v_c very precisely and being able to tune v_1 accurately. For typical alloy composition and values of v_c on the order of $1 \mu\text{m}/\text{sec}$ or less, the ratio $(\Gamma v_c/m_E C_\infty [1 - K_E] D_L)^{1/3}$ is on the order of $10^{-3} - 10^{-2}$ and the diffusion time is on the order of several minutes to an hour. Since, in the regime in which Eq. (1) is valid, $t_A \gg \tau_D$, experiments of very long duration would be required.

For typical alloy compositions the above practical difficulties cannot easily be overcome. However, by using an extremely dilute solution it is possible to make simultaneously the ratio $(\Gamma v_c/m_E C_\infty [1 - K_E] D_L)^{1/3}$ of order unity, v_c considerably larger (in the $20 - 100 \mu\text{m}/\text{sec}$ range), and the diffusion time D_L/v_c^2 considerably shorter ($\sim \text{sec}$). Using the material parameters of the SCN-acetone system, one can estimate that the above conditions would be met for acetone composition below about 0.01 wt%. So far, the smallest composition used in a controlled experiment is about an order of magnitude larger [26] and the control of the purity of the sample may be a limiting factor.

Another interesting possibility is to use liquid-crystal systems [34-37]. For example, in the 8CB-1.2% mole hexachloroethane alloy studied in Ref. [36] the ratio $(\Gamma v_c/m_E C_\infty [1 - K_E] D_L)^{1/3}$ is of order unity, $v_c \simeq 16 \mu\text{m}/\text{sec}$, and $D_L/v_c^2 \simeq 1.5 \text{ sec}$ (8CB denotes 4-*n*-octyl-4'-cyanobiphenyl). However, for this system, elastic effects which are not included in the present theory may play an important role. An indication that these effects may be important is the fact that a value of surface energy (γ) two to three orders of magnitude larger than the bare physical value (which is very small due to the fact that the nematic-isotropic transition is only weakly first order) has to be used [37] in order for the value of v_c predicted from linear stability analysis to match experiment. A treatment of morphological instability in this system that includes elastic effects and predicts v_c in terms of basic physical constants seems to be first required before extending the present treatment of fluctuation.

Finally, we remark that our present analysis is for a

spatially extended two-dimensional planar interface and does not take into account the effect of finite sample thickness. This effect can become relevant in experiments where the sample thickness W is comparable to or smaller than λ_c . A rough theoretical estimate yields that the value of F in Eq. (115) should be increased by a factor of λ_c/W in the limit $W \ll \lambda_c$.

ACKNOWLEDGMENTS

I wish to thank Jim Langer and Pierre Hohenberg for fruitful discussions in the early stage of this work and Chaouqi Misbah for critical reading of a first version of this manuscript and valuable comments. This research was supported by DOE Grant No. DE-FG02-92ER45471, in part by the Donors of the Petroleum Research Fund administered by ACS, and in part by NSF Grant No. PHY89-04035 during a visit at the Institute for Theoretical Physics in Santa Barbara.

APPENDIX A: EQUILIBRIUM FLUCTUATIONS IN THE TWO-SIDED MODEL

It is convenient to define the reduced composition fields in the two phases

$$u_\nu = \frac{C_\nu - C_\nu^0}{\Delta C^0}, \quad \nu = L, S \quad (\text{A1})$$

with $C_L^0 = C_\infty$, $C_S^0 = K_E C_\infty$, and $\Delta C^0 = (1 - K_E)C_\infty$. The interface boundary conditions become

$$u_L(\mathbf{p}) = -\frac{\Gamma}{m_E \Delta C^0} \kappa, \quad (\text{A2})$$

with $u_S(\mathbf{p}) = K_E u_L(\mathbf{p})$, and

$$v_n = \hat{\mathbf{n}} \cdot [D_S \nabla u_S - D_L \nabla u_L]. \quad (\text{A3})$$

$$+ \frac{1}{\Delta C^0} \hat{\mathbf{n}} \cdot [\mathbf{q}^L(\mathbf{p}) - \mathbf{q}^S(\mathbf{p})]. \quad (\text{A4})$$

The boundary integral formulation of Eq. (19) takes the form (in each phase, respectively)

$$\begin{aligned} \frac{u_L(\mathbf{p})}{2} &= D_L \int dt' \int d\mathbf{S}' [u_L(\mathbf{p}') \hat{\mathbf{n}}' \cdot \nabla' G_L(\mathbf{p}|\mathbf{p}') - G_L(\mathbf{p}|\mathbf{p}') \hat{\mathbf{n}}' \cdot \nabla' u_L(\mathbf{p}')] \\ &\quad - \int dt' \int d^2 r' u_L(\mathbf{p}') \frac{\partial \xi}{\partial t'} G_L(\mathbf{p}|\mathbf{p}') - \int dt' \int d^2 r' dz' G_L(\mathbf{p}|\mathbf{R}') \frac{1}{\Delta C^0} \nabla' \cdot \mathbf{q}^L(\mathbf{R}', t'), \end{aligned} \quad (\text{A5})$$

$$\begin{aligned} \frac{u_S(\mathbf{p})}{2} &= -D_S \int dt' \int d\mathbf{S}' [u_S(\mathbf{p}') \hat{\mathbf{n}}' \cdot \nabla' G_S(\mathbf{p}|\mathbf{p}') - G_S(\mathbf{p}|\mathbf{p}') \hat{\mathbf{n}}' \cdot \nabla' u_S(\mathbf{p}')] \\ &\quad + \int dt' \int d^2 r' u_S(\mathbf{p}') \frac{\partial \xi}{\partial t'} G_S(\mathbf{p}|\mathbf{p}') - \int dt' \int d^2 r' dz' G_S(\mathbf{p}|\mathbf{R}') \frac{1}{\Delta C^0} \nabla' \cdot \mathbf{q}^S(\mathbf{R}', t'), \end{aligned} \quad (\text{A6})$$

with the diffusion Green's function

$$G_\nu(\mathbf{R}|\mathbf{R}') \equiv \frac{1}{[4\pi D_\nu(t-t')]^{3/2}} \exp\left(-\frac{|\mathbf{r}-\mathbf{r}'|^2 + [z-z']^2}{4D_\nu(t-t')}\right). \quad (\text{A7})$$

We then linearize Eqs. (A5) and (A6) about a planar interface. A major simplification comes from the fact that terms involving the products $u_\nu \hat{\mathbf{n}} \cdot \nabla G_\nu$ and $u_\nu \frac{\partial \xi}{\partial t}$ do not contribute at linear order. We obtain

$$\frac{\Gamma}{2m_E \Delta C^0} \nabla_\perp^2 \xi(\mathbf{r}, t) = -\frac{\sigma^L(\mathbf{r}, t)}{\Delta C^0} - D_L \int_{-\infty}^t \frac{dt'}{[4\pi D_L(t-t')]^{3/2}} \int d^2 r' \exp\left(-\frac{|\mathbf{r}-\mathbf{r}'|^2}{4D_L(t-t')}\right) \partial_{z'} u_L(\mathbf{p}'), \quad (\text{A8})$$

$$\frac{K_E \Gamma}{2m_E \Delta C^0} \nabla_\perp^2 \xi(\mathbf{r}, t) = -\frac{\sigma^S(\mathbf{r}, t)}{\Delta C^0} + D_S \int_{-\infty}^t \frac{dt'}{[4\pi D_S(t-t')]^{3/2}} \int d^2 r' \exp\left(-\frac{|\mathbf{r}-\mathbf{r}'|^2}{4D_S(t-t')}\right) \partial_{z'} u_S(\mathbf{p}'), \quad (\text{A9})$$

with

$$\sigma^\nu(\mathbf{r}, t) = \int_{-\infty}^t \frac{dt'}{[4\pi D_\nu(t-t')]^{3/2}} \int d^2 r' dz' \exp\left(-\frac{|\mathbf{r}-\mathbf{r}'|^2 + z'^2}{4D_\nu(t-t')}\right) \nabla' \cdot \mathbf{q}^\nu(\mathbf{R}', t'). \quad (\text{A10})$$

The integral over z' in the last equation runs from 0 to ∞ in the liquid and from $-\infty$ to 0 in the solid. The next step consists in solving the above linear integral equations by Fourier transform. To do this we define the intermediate field

$$\Psi^\nu(\mathbf{r}, t) = \partial_z u_\nu(\mathbf{p}) = \partial_z u_\nu(x, y, z)|_{z=0} \quad (\text{A11})$$

and the Fourier transforms

$$\begin{pmatrix} \xi(\mathbf{r}, t) \\ \sigma_{\mathbf{k}\omega}^\nu(\mathbf{r}, t) \\ \Psi^\nu(\mathbf{r}, t) \end{pmatrix} = \frac{1}{(2\pi)^3} \int d\omega d^2k e^{i(\mathbf{k}\cdot\mathbf{r}+\omega t)} \begin{pmatrix} \xi_{\mathbf{k}\omega} \\ \sigma_{\mathbf{k}\omega}^\nu \\ \Psi_{\mathbf{k}\omega}^\nu \end{pmatrix}. \quad (\text{A12})$$

The transforms of Eqs. (A8) and (A9) together with that of the mass conservation condition

$$i\omega \xi_{\mathbf{k}\omega} = D_S \Psi_{\mathbf{k}\omega}^S - D_L \Psi_{\mathbf{k}\omega}^L + \frac{1}{\Delta C_0} [q_z^L(\mathbf{k}, \omega, 0) - q_z^S(\mathbf{k}, \omega, 0)] \quad (\text{A13})$$

give three algebraic equations for $\xi_{\mathbf{k}\omega}$, $\Psi_{\mathbf{k}\omega}^S$, and $\Psi_{\mathbf{k}\omega}^L$. Eliminating the last two variables and solving for $\xi_{\mathbf{k}\omega}$, we obtain after lengthy algebraic manipulations

$$\langle \xi_{\mathbf{k}\omega} \xi_{\mathbf{k}'\omega'} \rangle = \frac{4 [D_L^2 (Z_{\mathbf{k}\omega}^L Z_{\mathbf{k}'\omega'}^L)^{1/2} \langle B_{\mathbf{k}\omega}^L B_{\mathbf{k}'\omega'}^L \rangle + D_S^2 (Z_{\mathbf{k}\omega}^S Z_{\mathbf{k}'\omega'}^S)^{1/2} \langle B_{\mathbf{k}\omega}^S B_{\mathbf{k}'\omega'}^S \rangle]}{S_{\mathbf{k}\omega} S_{\mathbf{k}'\omega'}}, \quad (\text{A14})$$

with

$$S_{\mathbf{k}\omega} = \left[D_L (Z_{\mathbf{k}\omega}^L)^{1/2} + K_E D_S (Z_{\mathbf{k}\omega}^S)^{1/2} \right] \frac{\Gamma k^2}{m_E} + C_\infty (1 - K_E) i\omega, \quad (\text{A15})$$

$$Z_{\mathbf{k}\omega}^\nu = k^2 + i\omega/D_\nu, \quad (\text{A16})$$

$$\begin{aligned} \langle B_{\mathbf{k}\omega}^\nu B_{\mathbf{k}'\omega'}^\nu \rangle &= F^\nu \frac{(2\pi)^3 \delta(\mathbf{k} + \mathbf{k}') \delta(\omega + \omega')}{8 D_\nu^2 \text{Re}[(Z_{\mathbf{k}\omega}^\nu)^{1/2}]} \\ &\times \left(1 + \frac{\text{Re}[Z_{\mathbf{k}\omega}^\nu]}{(Z_{\mathbf{k}\omega}^\nu Z_{\mathbf{k}'\omega'}^\nu)^{1/2}} \right), \quad (\text{A17}) \end{aligned}$$

$F^L = 2D_L C_\infty$, and $F^S = 2K_E D_S C_\infty$. After further manipulations, $\langle \xi_{\mathbf{k}\omega} \xi_{\mathbf{k}'\omega'} \rangle$ can then be expressed in the more compact form

$$\begin{aligned} \langle \xi_{\mathbf{k}\omega} \xi_{\mathbf{k}'\omega'} \rangle &= (2\pi)^3 \delta(\mathbf{k} + \mathbf{k}') \delta(\omega + \omega') \frac{2 m_E C_\infty}{\Gamma k^2} \\ &\times \text{Re} \left[\frac{1}{S_{\mathbf{k}\omega}} \right], \quad (\text{A18}) \end{aligned}$$

which yields at once the results of Eqs. (31) and (32).

One technical point should be mentioned. To calculate $\sigma_{\mathbf{k}\omega}^\nu$ it is useful to separate the components of the bulk force parallel and perpendicular to the z axis by writing

$$\mathbf{q}^\nu(\mathbf{R}, t) = \mathbf{q}_\perp^\nu(\mathbf{R}, t) + \hat{\mathbf{z}} q_z^\nu(\mathbf{R}, t). \quad (\text{A19})$$

After Fourier transforming Eq. (A10), we obtain

$$\begin{aligned} \sigma_{\mathbf{k}\omega}^\nu &= \int_0^\infty \frac{d\tau}{(4\pi D_\nu \tau)^{1/2}} \int_0^\infty dz' \\ &\times \exp \left[-(D_\nu k^2 + i\omega) \tau - \frac{z'^2}{4D_\nu \tau} \right] \\ &\times [i\mathbf{k} \cdot \mathbf{q}_\perp^\nu(\mathbf{k}, \omega, z') + \partial_{z'} q_z^\nu(\mathbf{k}, \omega, z')]. \quad (\text{A20}) \end{aligned}$$

Integration by parts of the term $\partial_{z'} q_z^\nu(\mathbf{k}, \omega, z')$ in the last equation yields two boundary contributions (one for each phase) involving the term $q_z^\nu(\mathbf{k}, \omega, 0)$ which are canceled exactly by the boundary contributions associated with the term in square brackets on the right-hand side of Eq. (A13).

APPENDIX B: FLUCTUATIONS OF A MOVING PLANAR INTERFACE IN THE ONE-SIDED MODEL OF DIRECTIONAL SOLIDIFICATION

As in Appendix A, we define the field

$$u \equiv \frac{C_L - C_L^0}{\Delta C_0} \quad (\text{B1})$$

with the main difference that now $C_L^0 = C_\infty/K_E$, $\Delta C_0 = C_\infty(1/K_E - 1)$, and \mathbf{p} [\mathbf{p}'] denotes a point on the interface with coordinate $z = \xi(\mathbf{r}, \mathbf{t})$ [$z = \xi(\mathbf{r}', \mathbf{t}')$] in a frame moving with the interface. The interface conditions become

$$u(\mathbf{p}) = -\frac{\xi}{l_T} - d_0^c \kappa, \quad (\text{B2})$$

$$\begin{aligned} [1 + (1 - K_E)u(\mathbf{p})] \left[v + \frac{\partial \xi}{\partial t} \right] \hat{\mathbf{n}} \cdot \hat{\mathbf{z}} \\ = -D_L \hat{\mathbf{n}} \cdot \nabla u(\mathbf{p}) + \frac{1}{\Delta C_0} \hat{\mathbf{n}} \cdot \mathbf{q}^L(\mathbf{p}). \quad (\text{B3}) \end{aligned}$$

The boundary integral formulation of Eqs. (78) and (79) takes the form

$$\begin{aligned} 1 + \frac{u(\mathbf{p})}{2} &= D_L \int dt' \int d\mathbf{S}' [u(\mathbf{p}') \hat{\mathbf{n}}' \cdot \nabla' G(\mathbf{p}|\mathbf{p}') - G(\mathbf{p}|\mathbf{p}') \hat{\mathbf{n}}' \cdot \nabla' u(\mathbf{p}')] \\ &- \int dt' \int d^2r' u(\mathbf{p}') \left(v + \frac{\partial \xi}{\partial t'} \right) G(\mathbf{p}|\mathbf{p}') - \int dt' \int d^2r' dz' G(\mathbf{p}|\mathbf{R}') \frac{1}{\Delta C_0} \nabla' \cdot \mathbf{q}^L(\mathbf{R}', t'), \quad (\text{B4}) \end{aligned}$$

with the diffusion Green's function in the moving frame

$$G(\mathbf{R}|\mathbf{R}') \equiv \frac{1}{[4\pi D_L(t-t')]^{3/2}} \exp\left(-\frac{|\mathbf{r}-\mathbf{r}'|^2 + [z-z' + v(t-t')]^2}{4D_L(t-t')}\right). \quad (\text{B5})$$

Linearizing Eq. (B4) we obtain

$$\begin{aligned} -\left(\frac{1}{l_T} - d_0^c \nabla_{\perp}^2\right) \xi(\mathbf{r}, t) &= -\frac{\sigma(\mathbf{r}, t)}{\Delta C_0} + \int_{-\infty}^t \frac{dt'}{[4\pi D_L(t-t')]^{3/2}} \int d^2 r' \exp\left(-\frac{|\mathbf{r}-\mathbf{r}'|^2 + [v(t-t')]^2}{4D_L(t-t')}\right) \\ &\times \left[\frac{\partial \xi(\mathbf{r}', t')}{\partial t'} - \frac{v^2}{2D_L} \{\xi(\mathbf{r}, t) - \xi(\mathbf{r}', t')\} \right. \\ &\left. - v \left(\frac{1}{2} - K_E\right) \left(\frac{1}{l_T} - d_0^c (\nabla'_{\perp})^2\right) \xi(\mathbf{r}', t') - \frac{1}{\Delta C_0} q_z^L(\mathbf{p}) \right], \quad (\text{B6}) \end{aligned}$$

with

$$\sigma(\mathbf{r}, t) = \int_{-\infty}^t \frac{dt'}{[4\pi D_L(t-t')]^{3/2}} \int d^2 r' dz' \exp\left(-\frac{|\mathbf{r}-\mathbf{r}'|^2 + [z'-v(t-t')]^2}{4D_L(t-t')}\right) \nabla' \cdot \mathbf{q}^L(\mathbf{R}', t'). \quad (\text{B7})$$

The fluctuation spectrum is calculated by Fourier transforming Eqs. (B6) and (B7). The analog of Eq. (A20) becomes

$$\begin{aligned} \sigma_{\mathbf{k}\omega} &= \int_0^{\infty} \frac{d\tau}{(4\pi D_L \tau)^{1/2}} \int_0^{\infty} dz' \exp\left[\frac{v}{2D_L} z'\right] \\ &\times \exp\left[-(D_L k^2 + i\omega + v^2/4D_L)\tau - \frac{z'^2}{4D_L \tau}\right] [i\mathbf{k} \cdot \mathbf{q}_{\perp}^L(\mathbf{k}, \omega, z') + \partial_{z'} q_z^L(\mathbf{k}, \omega, z')], \quad (\text{B8}) \end{aligned}$$

with

$$\langle q_z^L(\mathbf{k}, \omega, z') q_z^L(\mathbf{k}, \omega, z'') \rangle_v = F(z') (2\pi)^3 \delta(\mathbf{k} + \mathbf{k}') \delta(\omega + \omega') \delta(z' - z'') \quad (\text{B9})$$

and

$$F(z') = 2D_L C_{\infty} (1/K_E - 1) \exp(-v z'/D_L) + C_{\infty}. \quad (\text{B10})$$

As before, the boundary contribution originating from integration by parts over z' of Eq. (B8) is canceled exactly by the contribution of the last term inside the square brackets on the right-hand side of Eq. (B6).

-
- [1] M. C. Cross and P. C. Hohenberg, *Rev. Mod. Phys.* **65**, 851 (1993).
[2] R. Pieters and J. S. Langer, *Phys. Rev. Lett.* **56**, 1948 (1986).
[3] P. Pelce, thèse, Université de Provence, Marseille, 1986.
[4] M. Barber, A. Barbieri, and J. S. Langer, *Phys. Rev. A* **36**, 3340 (1987).
[5] J. S. Langer, *Phys. Rev. A* **36**, 3350 (1987).
[6] D. Kessler and H. Levine, *Europhys. Lett.* **4**, 215 (1987).
[7] B. Caroli, C. Caroli, and B. Roulet, *J. Phys. (Paris)* **48**, 1423 (1987).
[8] C. Huang and M. E. Glicksman, *Acta Metall.* **29**, 701 (1981); **29** 717 (1981).
[9] A. Dougherty, P. D. Kaplan, and J. P. Gollub, *Phys. Rev. Lett.* **58**, 1652 (1987).
[10] Experiments exist where sidebranching seems to result from a well-marked oscillatory behavior of the dendrite tip: L. R. Morris and W. C. Winegard, *J. Cryst. Growth* **1**, 245 (1967); H. Honjo, S. Ohta, and Y. Sawada, *Phys. Rev. Lett.* **56**, 2032 (1986).
[11] J. A. Warren and J. S. Langer, *Phys. Rev. E* **47**, 2702 (1993).
[12] R. Trivedi and K. Somboonsuk, *Acta Metall.* **33**, 1061 (1985).
[13] K. Somboonsuk, J. T. Mason, and R. Trivedi, *Metall. Trans.* **15A**, 967 (1984).
[14] J. Bechhoefer and A. Libchaber, *Phys. Rev. B* **35**, 1393 (1987).
[15] H. Chou and H. Z. Cummins, *Phys. Rev. Lett.* **61**, 173 (1988).
[16] X. W. Qian, H. Chou, M. Muschol, and H. Z. Cummins, *Phys. Rev. B* **39**, 2529 (1989).
[17] H. Z. Cummins, G. Livenu, H. Chou, and M. R. Srinivasan, *Solid State Commun.* **60**, 857 (1986).
[18] J.-M. Laherrere, H. Savary, R. Mellet, and J.-C. Tolenado, *Phys. Rev. A* **41**, 1142 (1990).
[19] J. S. Langer, *Rev. Mod. Phys.* **52**, 1 (1980).
[20] A. Karma, *Phys. Rev. Lett.* **70**, 3439 (1993).
[21] W. W. Mullins and R. F. Sekerka, *J. Appl. Phys.* **35**, 444 (1964).
[22] T. A. Cherepanova, *Dokl. Akad. Nauk. SSSR* **226**, 1066 (1976) [*Sov. Phys. Dokl.* **21**, 109 (1976)].
[23] Y. Wu., T. J. Piccone, Y. Shiohara, and M. C. Flemmings, *Metall. Trans.* **18A**, 925 (1987).
[24] S. R. Coriell and D. Turnbull, *Acta Metall.* **30**, 2135 (1982).
[25] A.-M. S. Tremblay, E. D. Siggia, and M. R. Arai, *Phys. Lett.* **76A**, 57 (1980); A.-M. S. Tremblay, M. Arai, and E. D. Siggia, *Phys. Rev. A* **23**, 1451 (1981).
[26] M. A. Eshelman and R. Trivedi, *Acta Metall.* **35**, 2443 (1987); *Scr. Metall.* **22**, 893 (1988).
[27] G. Ahlers, M. C. Cross, P. C. Hohenberg, and S. Safran,

- J. Fluid Mech. **110**, 297 (1981).
- [28] P. C. Hohenberg and J. B. Swift, Phys. Rev. A **46**, 4773 (1992).
- [29] L. D. Landau and E. M. Lifshitz, *Statistical Physics* (Pergamon, New York 1980).
- [30] W. Kurz and D. J. Fisher, *Fundamentals of Solidification* (Trans Tech, Switzerland, 1989).
- [31] In certain limits, we were able to show explicitly that this integral equals unity by extending it in the complex plane and evaluating the residues taking care of various branch cuts. For the general case, we have evaluated it numerically and found that it always equals unity for all the parameter values that were tried.
- [32] J. S. Rowlinson and B. Widom, *Molecular Theory of Capillarity* (Clarendon Press, Oxford, 1982).
- [33] B. Caroli, C. Caroli, and L. Ramirez-Piscina (unpublished).
- [34] B. Caroli, C. Caroli, and B. Roulet, J. Phys. (Paris) **43**, 1767 (1982).
- [35] P. Oswald, J. Bechhoefer, and A. Libchaber, Phys. Rev. Lett. **58**, 2318 (1987).
- [36] A. J. Simon, J. Bechhoefer, and A. Libchaber, Phys. Rev. Lett. **61**, 2574 (1988).
- [37] J. Bechhoefer, Ph.D. thesis, University of Chicago, 1988.